ELSEVIER

Coordination Chemistry Reviews
193–195 (1999) 1069–1117

COORDINATION CHEMISTRY REVIEWS

www.elsevier.com/locate/ccr

Coordination chemistry of *N*,*N*′-bis(coordinating group substituted)oxamides: a rational design of nuclearity tailored polynuclear complexes

Rafael Ruiz [a], Juan Faus [a], Francesc Lloret [a,1], Miguel Julve [a,*], Y. Journaux [b]

[a] *Departament de Química Inorgànica, Facultat de Química de la Universitat de València, Dr. Moliner 50, 46100 Burjassot, València, Spain*

[b] *Laboratoire de Chimie Inorganique, Université de Paris-Sud, UMR 8613 CNRS, 91420 Orsay, France*

Received 7 January 1999; accepted 16 April 1999

Contents

---

* Corresponding author. Tel.: +34-96-3983001; fax: +34-96-3864322.
E-mail address: miguel.julve@uv.es (M. Julve)

[1] Also corresponding author.

PII: S0010-8545(99)00138-1

Abstract

The coordinating properties of *N*,*N*′-bis(coordinating group substituted)oxamides have been thoroughly investigated both in aqueous solution and in the solid state. The easy *cis–trans* isomerization equilibria that they exhibit together with the great variety of *N*,*N*′-substituents which can be used to play on the overall charge, complexing ability and polarity, make them very suitable ligands in designing homo- and heterometallic species. The knowledge of their complex formation in aqueous solution by potentiometry and using the hydrogen ion concentration as a probe, allowed us to settle the basis of a rational design of oxamidate-containing polynuclear species whose nuclearity can be easily tuned. Concerning their electronic properties, the strong basicity of the deprotonated amide–nitrogen atoms stabilizes high oxidation states of late first-row transition metal ions. Finally, one of the most appealing aspects of this type of ligands is the remarkable efficiency they exhibit to mediate strong antiferromagnetic interactions between paramagnetic centres when acting as bridges but in order to maintain the present work within a rational length, we have omitted this last point which deserves a further review.

Keywords: Oxamidate complexes; Stability constants; Polynuclear complexes; Homometallic complexes; Heterometallic complexes; High oxidation states.

1. Introduction

Oxamide dianion ($HNCOCONH^{2-}$, Scheme 1) can adopt bidentate and bis-bidentate coordination modes in its metal complexes, like the parent oxalate, to yield either mono- [1–5]or polynuclear [6–13] compounds. The strong electron-donating capability of its deprotonated nitrogen–amide atoms accounts for the greater stability of its metal complexes when comparing with that of the oxalato ones. This great basicity is also responsible for the stabilization of high oxidation states such as Cu(III) and Ni(III) [14]. Moreover, the lower electronegativity of the nitrogen atoms respect to the oxygen ones allows stronger magnetic interactions between metal centres through oxamidato bridges when comparing to the same situation in oxalato-bridged compounds [7,10,11]. However, the insolubility of oxamide in common solvents and the hydrolytic reaction it undergoes under deprotonation to yield oxalate [5,11,12] (Scheme 1) preclude an exhaustive exploration of its coordination chemistry.

These difficulties can be overcome by using *N*,*N*′-bis(coordinating group substituted)oxamides (Scheme 2). They are more reluctant towards the hydrolytic reaction and their solubility can be much increased by choosing the appropriate substituent. Furthermore, in the presence of metal ions and when the oxamide has another coordinating group at a position which can form five- or six-membered chelate rings, the amide group deprotonates and coordinates simultaneously in a

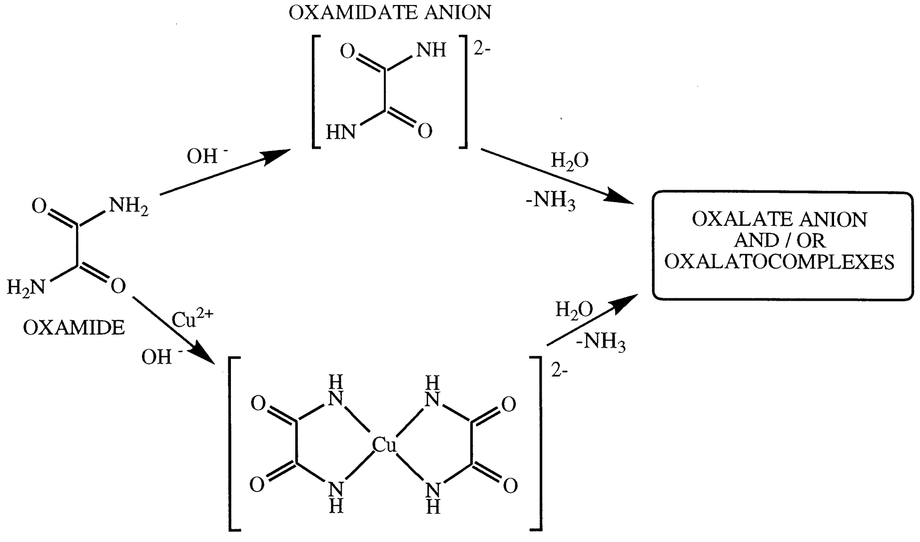

Scheme 1.

low pH range as noted in a previous review on copper(II) complexes with *N*,*N*′-bis(substituent)oxamides [15]. We have taken this review as starting point to illustrate the applicability of these versatile ligands in designing homo- and heterometallic complexes with new properties. The synthetic strategies that we have developed to prepare polynuclear species whose nuclearity can be tuned, and the information that we and others have got both in solution and in the solid state constitute the heart of the present contribution.

2. *N*,*N*′-bis(coordinating group substituted oxamides)

2.1. Synthetic strategies

The general preparative route to these oxamide ligands consists of reacting either ethyloxalate or oxalylchloride with the appropriate amine derivatives such as shown

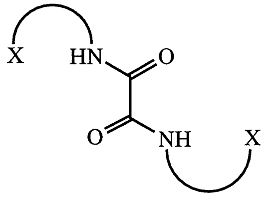

$X = NR_2$, py, OH, COO^-, SO_3^-

Scheme 2.

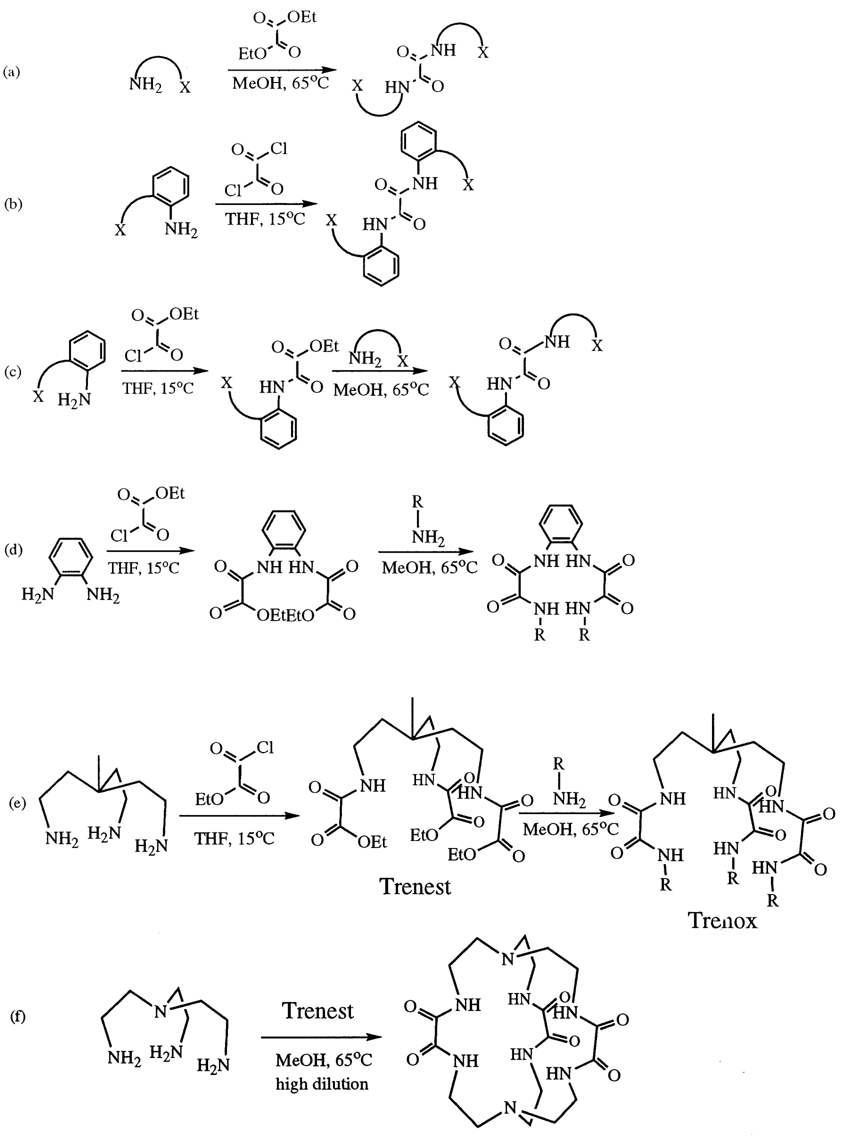

Scheme 3.

in Scheme 3(a–f). The great variety of oxamides available through these high yield simple synthetic routes together with their remarkable versatility as ligands, makes them a very interesting family in coordination chemistry. The overall charge, polarity, coordinating capability and solubility of the resulting substituted oxamide is strongly dependent on the nature of the X group. Finally, the asymmetric character of the ethyl oxalyl chloride and the different basicity of aromatic and

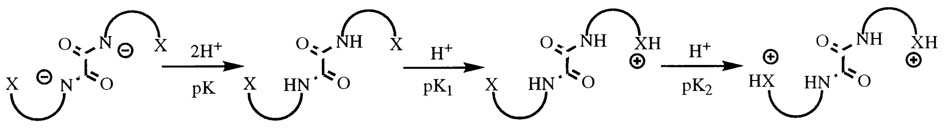

Scheme 4.

aliphatic amines render easy the design and preparation of asymmetric substituted mono- and polyoxamides (Scheme 3c) [16,17].

2.2. Acid–base properties

It is well known that the amide–nitrogen atom in a neutral common amide [(C=O)NHR] has no basic character because the electron withdrawing character of the adjoining carbonyl oxygen atom. However, it can act as a very weak acid in aqueous solution by proton dissociation (pK_a (C=O)NHR ~13–15) [18]. Consequently, common amides are neutral in a wide pH range. As far as the *N*,*N*′-bis-(substituent)oxamides are concerned the following acid–base-equilibria (Scheme 4) are involved.

The first step corresponds with the protonation of the oxamidate dianion and is not influenced by the nature of the substituents on the amide–nitrogen atoms. A value of log β_2 close to 24 was obtained by potentiometry for all the oxamidate ligands which were investigated (Table 1, Scheme 5) [19–23]. The two last steps refer to the protonation of the X group and its value is mainly determined by the

Table 1
Equilibrium data for basicity and formation of Cu(II) complexes with oxamido ligands (L) in aqueous solution (25°C and 0.1 mol dm^{-3}, NaNO$_3$)

	log *K*					
Reaction	L = **1**	**2**	**3**	**4**	**6**	**8**
(1) $2H + L \rightleftarrows H_2L$	24.0	24.0	24.0	24.0	23.7	24.2
(2) $H + H_2L \rightleftarrows H_3L$	10.1	9.5	10.3	8.6	4.37	3.6
(3) $H + H_3L \rightleftarrows H_4L$	9.5	8.9	9.8	7.8	4.27	2.9
(4) $Cu + L \rightleftarrows [CuL]$	20.2	–	17.1	16.9	~17	–
(5) $Cu + H_2 \rightleftarrows [Cu(H_2L)]$	–	–	–	–	–	2.62
(6) $2Cu + H_2L \rightleftarrows [Cu_2(H_2L)]$	<10	10.64	12.7	10.1	<10	–
(7) $2Cu + H_2L \rightleftarrows [Cu_2(HL)] + H$	<5	5.12	7.7	5.5	<5	–
(8) $2Cu + L \rightleftarrows [Cu_2L]$	28.1	23.2	26.4	24.7	26.1	22.0
(9) $2Cu + L + OH \rightleftarrows [Cu_2L(OH)]$	–	14.7	–	–	–	–
(10) $2Cu + L + 2OH \rightleftarrows [Cu_2L(OH)_2]$	–	4.9	–	–	–	–
(11) $3Cu + 2L \rightleftarrows [Cu_3L_2]$	51.7	–	47.3	44.9	?	?
(12) $4Cu + 3L \rightleftarrows [Cu_4L_3]$	74.3	–	67.5	64.1	?	?

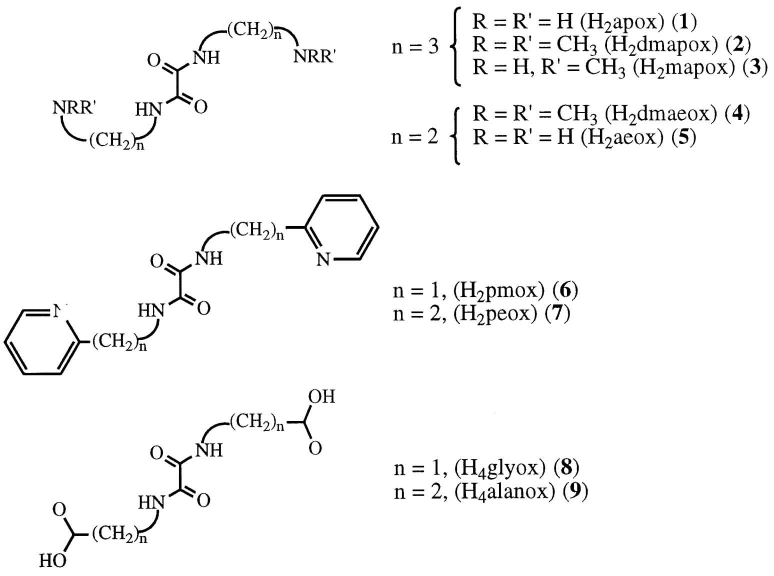

n = 3 { $R = R' = H$ (H_2apox) (**1**)
$R = R' = CH_3$ (H_2dmapox) (**2**)
$R = H, R' = CH_3$ (H_2mapox) (**3**)

n = 2 { $R = R' = CH_3$ (H_2dmaeox) (**4**)
$R = R' = H$ (H_2aeox) (**5**)

n = 1, (H_2pmox) (**6**)
n = 2, (H_2peox) (**7**)

n = 1, (H_4glyox) (**8**)
n = 2, (H_4alanox) (**9**)

Scheme 5.

nature of X. The corresponding proton affinity constants are also included in Table 1. The distribution diagrams for two selected examples [namely mapox (**3**) and glyox (**8**)] are depicted in Fig. 1a and 1b, respectively. As it can be seen in these plots, the deprotonation of the neutral oxamides H_2L to yield the fully deprotonated L^{2-} species only takes place at $pH > 11$. This dianion is the only existing species at $pH > 13$. The high value of the overall protonation constant of the oxamidate group (first step in Scheme 4, Eq. (1) from Table 1) illustrates the great basicity of this species and accounts for the difficulty associated to its determination by potentiometry. The trend observed in the values of the protonation constants of the X group (Eqs. (2) and (3) in Table 1) is as expected taking into account the different basicity of amine (**1**–**4**), pyridyl (**6**) and carboxylate (**8**) groups. The values of the logarithm of the stepwise protonation constants of the amine groups of H_2L (**1**–**4**) are within the range observed for aliphatic amines [24]. In the case of H_2glyox^{2-}, the values of the protonation constants of its two carboxylate groups are very close to those previously reported [25], and lie within the range observed for β-(electronegative group)-substituted carboxylic acids [24]. Finally, the value of the logarithm of the first protonation constant for the pyridyl groups of H_2pmox (**6**) ($\log K = 4.37$, Eq. (3) in Table 1) is significantly smaller than that reported for the parent 2-methylpyridine ($\log K = 6.06$) [26]. This is probably due to the occurrence of a hydrogen bond between the N–H amide group and the pyridyl–N atom which should be broken under deprotonation.

2.3. The cis–trans conformational change

The *N*,*N*′-bis(substituent)oxamides can adopt either the *cis* or *trans* conformation in its metal complexes (Scheme 6a). Ab initio calculations using the *N*,*N*′dimethyloxamidate $(CH_3NCO)_2^{2-}$ as model system (Scheme 6b) were carried out to evaluate the energy gap between both conformers [21,27,28]. In these calculations, the internal dihedral angle β (i.e. the twisting around the C–C bond)

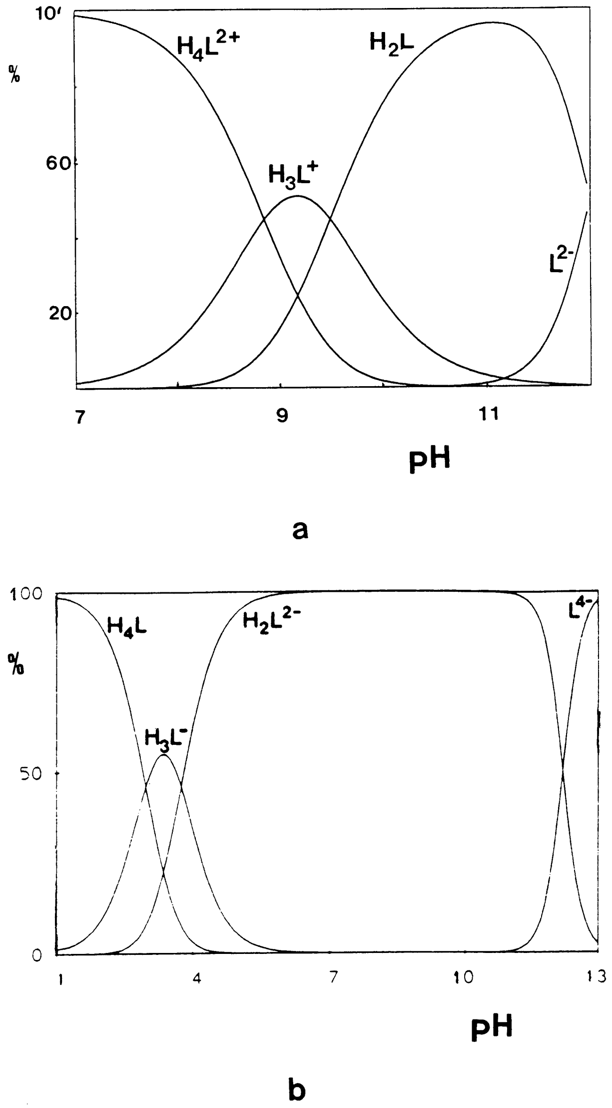

Fig. 1. Distribution diagrams for the systems (a) H^+–mapox^{2-} and (b) H^+–glyox^{4-}. (Reprinted with permission from Lloret et al. [20b, 22a]. Copyright © 1992 American Chemical Society.)

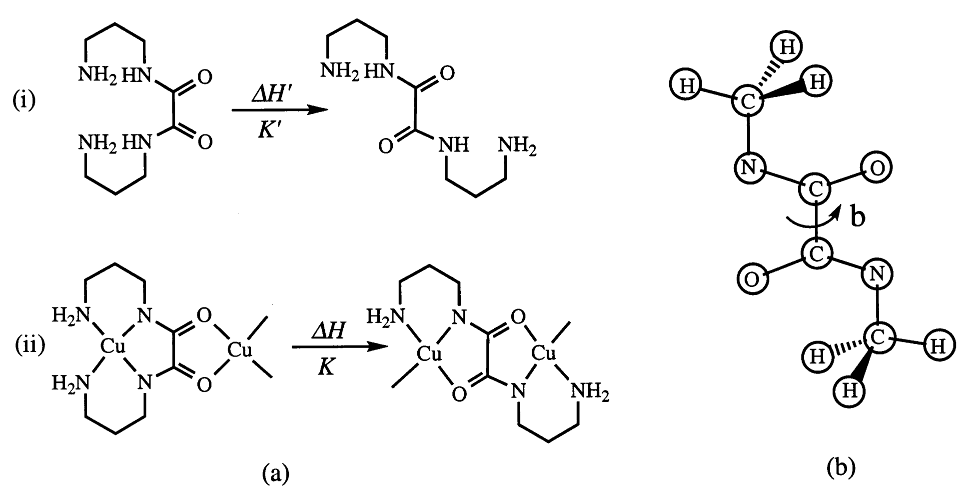

Scheme 6.

was varied between 0 and 180°. According to these calculations, the *cis* isomer lies 2.25 Kcal above the *trans* one at the DZ SCF level of theory.

3. Studies of complex formation with disubstituted monooxamides

3.1. *N,N'-bis(3-aminopropyl)oxamidate (apox) as ligand*

3.1.1. *Copper(II) complexes*

Potentiometric and spectrophotometric studies of the Cu(II)-apox^{2-} system showed the formation of mono-, di-, tri- and tetranuclear complexes whose stoichiometries and stability constants are listed in Table 1 (Eqs. (4)–(12)) [21]. The analysis of the potentiometric data was carried out by means of the SUPERQUAD and BEST programs [29,30]. An inspection of the distribution diagram of the system $Cu^{2+}-H_2apox$ (Fig. 2a, bottom), shows that the $[Cu_2(apox)]^{2+}$ dimeric complex is the only existing species in the pH range 5.5–6.5; the formation of the corresponding tri- and tetranuclear species only takes place at $pH > 6.5$. Finally, the neutral [Cu(apox)] mononuclear complex is the major species at $pH > 8.4$, and it becomes the only existing complex at $pH > 9.5$.

The stoichiometries of the different copper(II) complexes with apox as a function of pH are shown in Scheme 7(a,b,e). From an inspection of Table 1, two important

---

Fig. 2. Distribution diagrams for the systems $M^{2+}-Cu^{2+}-apox^{2-}-H^+$ (M = Cd, Zn, Mn, Co, Ni, Cu) as a function of (a) pH and (b) p[Cu(apox)]. $c_{[Cu(apox)]} = 1 \times 10^{-2}$ mol dm^{-3} and $[Cu(apox)]/[M^{2+}] = 3$ are common to all distribution diagrams except in the case of M = Cu (bottom, left) for which $c_{Cu^{2+}} = c_{H_2apox} > 10^{-2}$ mol dm^{-3}. 1–3 correspond to $\{M[Cu(apox)]\}^{2+}$, $\{M[Cu(apox)]_2\}^{2+}$, and $\{M[Cu(apox)]_3\}^{2+}$, respectively. All the percentages are referred to total concentration of M. (Reprinted with permission from Lloret et al. [21]. Copyright © 1992 American Chemical Society.)

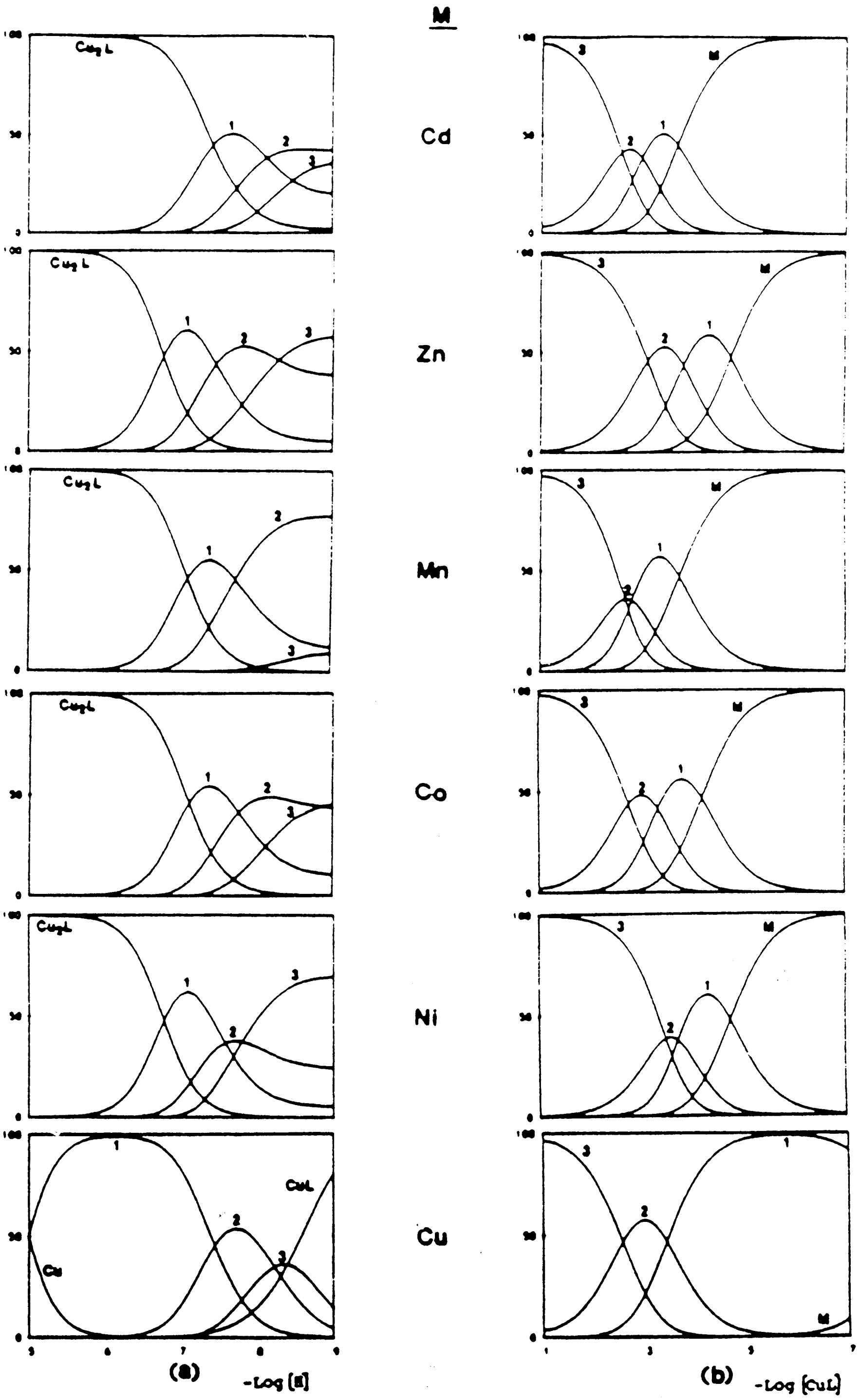
M
Cd
Zn
Mn
Co
Ni
Cu
Cu2L
CuL
Cu
1
2
3
M
100
50
0
5
6
7
8
9
1
3
5
7
(a)
-Log [E]
(b)
-Log [CuL]

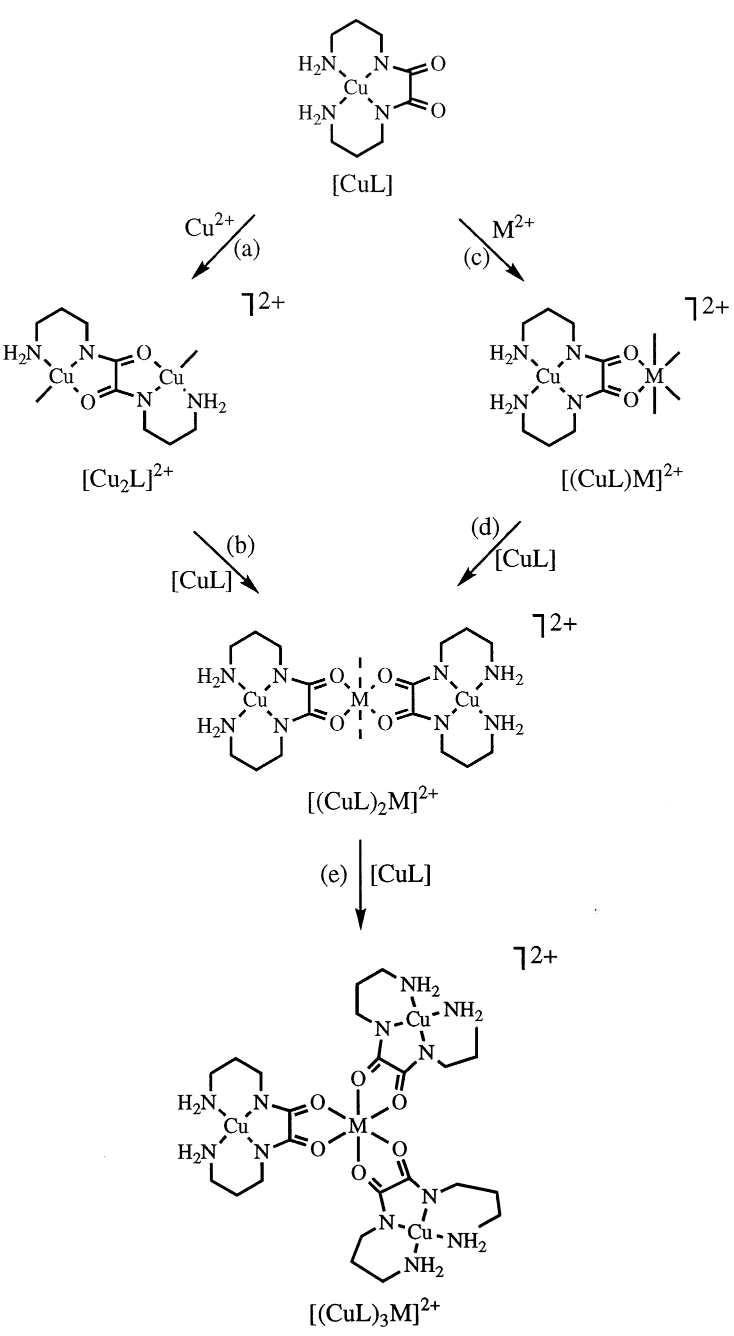

Scheme 7.

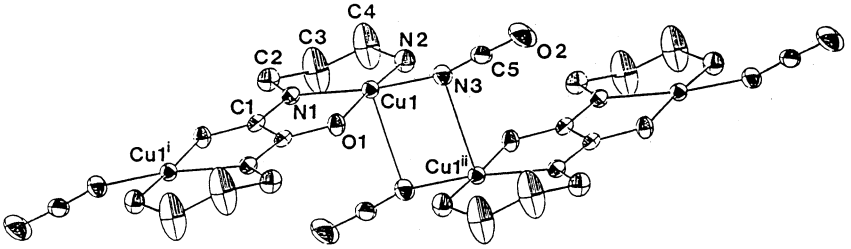

Fig. 3. Molecular structure of $[Cu_2(apox)(NCO)_2]$. (Reprinted with permission from Lloret et al. [21]. Copyright © 1992 American Chemical Society.)

points deserve to be discussed. The first one concerns the fact that the *N*,*N*′-bis(substituent)oxamides deprotonates and coordinates to the copper(II) in an unexpectedly low pH range. The occurrence of a coordinating group (amine or carboxylate) at a position which can form six- or five- membered chelate in the presence of metal ions accounts for this feature. The second one deals with the great stability of the copper(II) dimer $[Cu_2L]$ (L = **1**–**4**,**6**,**8**). This stability is so high that this kind of ligand is selective towards copper(II). Fig. 2b (bottom) illustrates the great stability of $[Cu_2(apox)]^{2+}$ respect to the other complexes: $[Cu_2(apox)]^{2+}$ is formed quantitatively in the range $5 < p[Cu(apox)] < 7$. The tetranuclear $[Cu_4(apox)_3]^{2+}$ species is the main one only at high concentrations of [Cu(apox)]. A comparison of the values of the stability constant of $[Cu_2L]$ (Eq. (8) in Table 1) shows that for L = apox [21] its value is two and six orders of magnitude greater than that observed when L = pmox [19] and glyox [20]. Two factors account for this stability trend: (a) two five-membered fused chelate rings around each copper(II) ion occur in $[Cu_2(pmox)]^{2+}$ and $[Cu_2(glyox)]$ whereas the more stable alternating five- and six-membered fused chelates are present in $[Cu_2(apox)]^{2+}$; (b) the set of donor atoms around each copper atom ($CuNO_2X$) in this dimeric species is different, X being amine–N (apox), pyridine–N (pmox) or carboxylate–O (glyox). The increasing stability trend of the Cu_2L species (glyox < pmox < apox) follows that of the affinity of copper(II) by carboxylate–O and pyridine– and amine–N atoms.

These solution studies are very important not only because of the determination of the stability constants of the metal complexes they afford, but also because they are precious for the synthetic chemist aiming at designing the best experimental conditions to carry out the preparation of the desired species. This is the case for the oxamidate-containing metal complexes of the present review. In this respect, the synthesis of the apox-containing copper(II) complexes was performed at the appropriate pH values where the maximum formation degree of the desired species occurs. For instance, the $[Cu_2(apox)]^{2+}$ binuclear complex was isolated from its aqueous solution at pH ca. 6 by adding the stoichiometric amount of cyanate [21], thiocyanate [31] or azide [32]. The structures of the resulting compounds of formula $[Cu_2(apox)(NCO)_2]$ (Fig. 3), $[Cu_2(apox)(NCS)_2(H_2O)]$ (Fig. 4) and $[Cu_2(apox)(N_3)_2(H_2O)_2]$ (Fig. 5) have in common the adoption of the *trans* conformation of the bridging oxamidate ligand. The copper surrounding is square

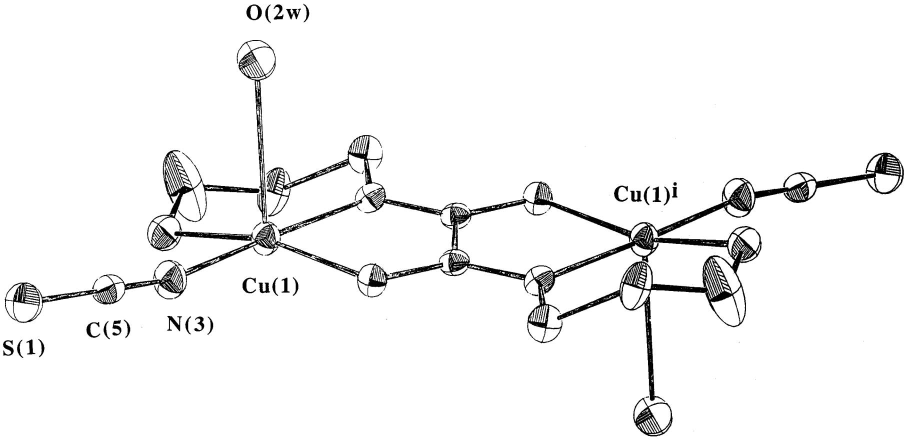

Fig. 4. Molecular structure of $[Cu_2(apox)(NCS)_2(H_2O)]$.

pyramidal in this family with a nitrogen atom from the pseudohalide ligand and one carbonyl–oxygen and the amine– and amide–nitrogen atoms from apox building the equatorial plane. A weakly coordinated water molecule occupies the axial position in the two last compounds whereas the cyanate–nitrogen from an adjacent unit fills this site in the first compound. The cyanate derivative is thus an alternating copper(II) chain where bis(terdentate) apox and di-μ-1,1-cyanato bridges alternate regularly within the chain.

The $[Cu_3(apox)_2]^{2+}$ trinuclear species was synthesized as a perchlorate salt from aqueous solutions containing Cu^{2+} and H_2apox at pH ca. 7.5 (that is at the pH value where the trimer is the dominant species as shown in Fig. 2a). In this trimeric species, the oxamidato ligand adopts the *cis* conformation as shown in Fig. 6 [33].

The [Cu(apox)] mononuclear complex is easily isolated from the corresponding aqueous solutions at pH > 9. Its crystal structure (Fig. 7) [34] shows how the oxamidate ligand acts as a tetradentate ligand coordinating to copper(II) through its four nitrogen atoms. The oxamidate adopts the *cis* conformation and forms 6–5–6 membered fused chelates around the copper atom.

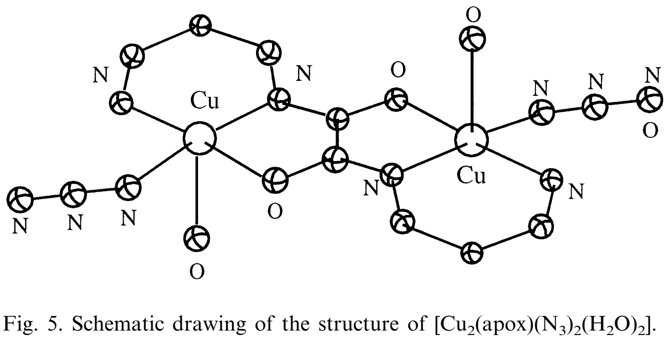

Fig. 5. Schematic drawing of the structure of $[Cu_2(apox)(N_3)_2(H_2O)_2]$.

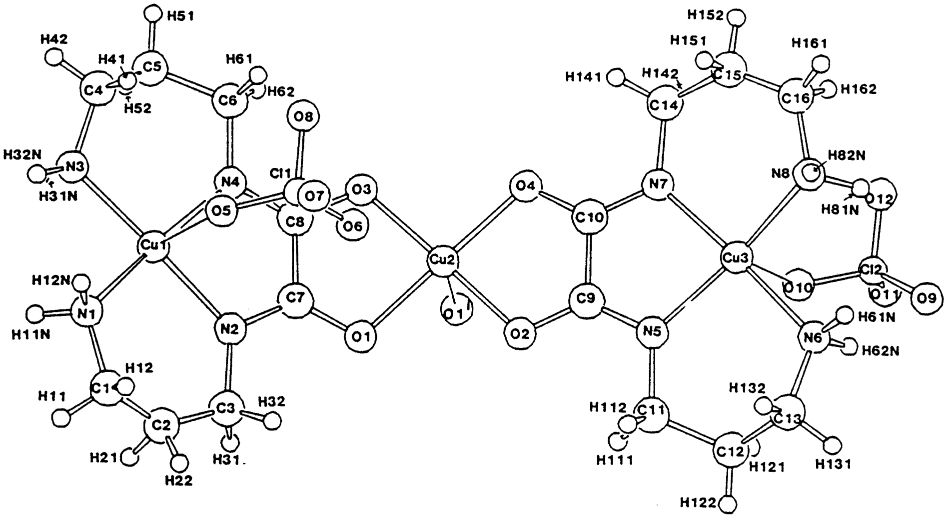

Fig. 6. Structure of $[Cu_3(apox)_2(ClO_4)_2]$. (Reprinted with permission from Journaux et al. [33]. Copyright © 1986 American Chemical Society.)

Finally, the $[Cu_4(apox)_3]^{2+}$ tetranuclear complex whose assumed structure is shown in Scheme 8 is a predominant species only at high concentrations of [Cu(apox)] (> 0.1 mol dm^{-3}) (Fig. 2a, bottom). Mixtures of tri- and tetranuclear apox-containing copper(II) complexes were obtained in our attempts to prepare this tetrameric compound. In fact, the low stability of this complex in water (see Table 1) together with the moderate solubility of the mononuclear precursor [Cu(apox)] make very difficult its isolation. Formally, the $[Cu_4(apox)_3]^{2+}$ tetramer would result from the coordination of [Cu(apox)] through its two carbonyl–oxygens to the central copper(II) ion of the $[Cu_3(apox]^{2+}$ trimer. The Jahn–Teller effect in the $Cu(II)O_6$ core of the tetramer is most likely the factor responsible for its low

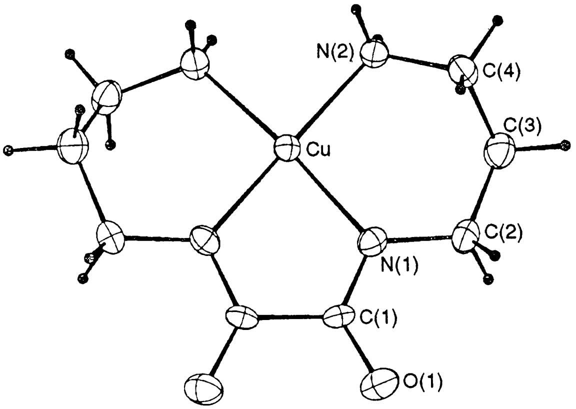

Fig. 7. Top view of the molecular structure of [Cu(apox)]. (Reproduced with permission from Sanz et al. [34]. Copyright © 1996 The Royal Society of Chemistry.)

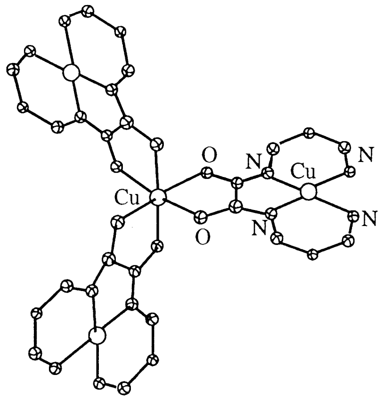

Scheme 8.

stability. The analysis of the influence of this effect and that of the *cis–trans* conformational change of apox on the stability constants of the corresponding metal complexes is done in Section 3.1.3.

Summarising, the versatility of the apox as ligand (tetradentate η^4, bis(terdentate) η^3:η^3, and tetradentate-bidentate η^4:η^2 coordination modes) is due to the easy *cis–trans* conformational change it undergoes. The variety of the species which can be designed and prepared by reaction of copper(II) with apox^{2-} is sketched in Scheme 7 (steps a, b and e with M = Cu).

3.1.2. Other homometallic complexes

N,*N*′-bis(coordinating group substituted)oxamides (H_2L) form copper(II) complexes so stable (Table 1) that they are selective ligands for this metal ion. However, this stability is much decreased when copper(II) is replaced by other divalent first-row transition metal ions. For instance, the corresponding metal hydroxides precipitate when aqueous solutions of H_2L and M(II) (M = VO^{2+}, Mn^{2+}, Fe^{2+}, Co^{2+} and Zn^{2+}) are titrated with sodium hydroxide. However, this problem was overcome by using imino or phenolate as exogenous groups in the oxamidate and even oxamidate-bridged dinuclear iron(III) or vanadium(IV) complexes could be prepared [35]. Nickel(II) is the only metal ion for which complex formation could be observed in aqueous solution [20], although the potentiometric measurements are difficult because of the slow conversion of the octahedral hexaaquo nickel(II) complex into the square planar oxamidate nickel(II) species [36–39]. The strong field ligand induced by the great basicity of the deprotonated amide–nitrogen atoms of the oxamidate accounts for the preferred square planar environment in the case of nickel(II). Anyway, the available values of stability constants for the $[Ni_2L]$ dinuclear species ($\log K = 18.5$ and 13.1 for $[Ni_2(apox)]^{2+}$ and $[Ni_2(glyox)]$, respectively) [20,21] reveal that they are much less stable species than the parent $[Cu_2L]$ ones ($\log K = 28.1$ and 22.0 for $[Cu_2(apox)]^{2+}$ and $[Cu_2(glyox)]$, respectively).

Table 2
Overall (β_n) and stepwise (K_n) stability constants concerning complex formation between [CuL] and M^{2+} in aqueous solution (25°C and 0.1 mol dm^{-3}, $NaNO_3$) (Reprinted with permission from Lloret et al. [21]. Copyright © 1992 American Chemical Society.)

	M = Mn	Co	Ni	Cu	Zn	Cd
log β_1	3.63	4.08	4.63	7.92	4.64	3.57
log β_2	6.33	7.31	8.24	11.22	8.35	6.44
log β_3	8.89	9.97	11.61	13.66	11.35	8.91
log K_1	3.63	4.08	4.63	7.92	4.64	3.57
log K_2	2.70	3.23	3.61	3.30	3.71	2.87
log K_3	2.26	2.66	3.37	2.44	3.00	2.47

3.1.3. Heterobimetallic complexes

The great stability of the [Cu(apox)] mononuclear complex and its capability to coordinate to metal ions as a bidentate ligand through the carbonyl–oxygen atoms make it a very suitable building block in designing heteropolymetallic species (see Scheme 7, steps c–e). Potentiometric studies on the ternary Cu^{2+}–M^{2+}-$apox^{2-}$ system (M = Mn, Co, Ni, Zn, Cd) [21] proved the formation of the expected di-, tri- and tetranuclear complexes (Eq. (1), $n = 1$–3)

$$n[\mathrm{Cu(apox)}] + \mathrm{M}^{2+} \leftrightarrow [\mathrm{M}\{\mathrm{Cu(apox)}\}_n] \quad (1)$$

Table 3
Species involved in the equilibria[a]: $p\mathrm{M}^{2+} + q\mathrm{Cu}^{2+} + r\mathrm{L}^{2-} \leftrightarrow [\mathrm{M}_p\mathrm{Cu}_q\mathrm{L}_r]^{2(p+q-r)}$

M^{2+}	Cu^{2+}	L^{2-}	log K
0	1	1	20.2
0	2	1	28.1
0	3	2	51.7
0	4	3	74.3
1 (Mn)	1	1	23.9
1 (Mn)	2	2	46.8
1 (Mn)	3	3	69.6
1 (Co)	1	1	24.3
1 (Co)	2	2	47.8
1 (Co)	3	3	70.7
1 (Ni)	1	1	24.9
1 (Ni)	2	2	48.7
1 (Ni)	3	3	72.3
1 (Zn)	1	1	24.9
1 (Zn)	2	2	48.8
1 (Zn)	3	3	72.0
1 (Cd)	1	1	23.8
1 (Cd)	2	2	46.9
1 (Cd)	3	3	69.6

[a] Values at 25°C and 0.1 mol dm^{-3}, $NaNO_3$.

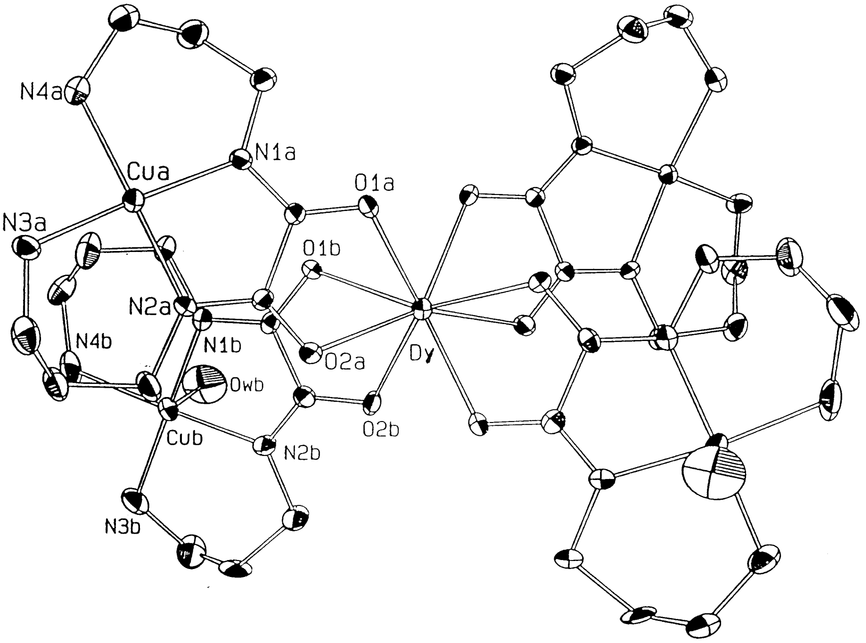

Fig. 8. Perspective view of the structure of the heteropentanuclear cation $\{Dy[Cu(apox)]_2[Cu(apox)(H_2O)]_2\}^{3+}$. (Reprinted with permission from Sanz et al. [42]. Copyright © 1996 American Chemical Society.)

The computed stability constants associated to Eq. (1) are listed in Table 2 whereas the overall stability constants are grouped in Table 3. The distribution diagrams showing the formation of these heteropolynuclear species (see Fig. 2) are very useful in visualizing the best conditions to isolate the desired heteropolynuclear compounds. For instance, the trinuclear $[M\{Cu(apox)\}_2]^{2+}$ and tetranuclear $[M\{Cu(apox)\}_3]^{2+}$ species were readily isolated by addition of an excess of sodium perchlorate to aqueous solutions containing the 2:1 and 3:1 [Cu(apox)]: M^{2+} molar ratio, respectively [33,40,41]. In these compounds, the neutral [Cu(apox)] unit acts as a bidentate ligand through its two carbonyl–oxygen atoms, the apox ligand exhibiting the *cis* conformation. This conformation is also kept in the pentanuclear $[Ln(III)\{Cu(apox)\}_4]^{3+}$ complex (Ln = Gd, Dy, Ho) (Fig. 8) [42] where eight carbonyl–oxygens from four [Cu(apox)] complex ligands build a pseudo-square-antiprismatic environment around the rare earth element.

A large family of $[ML'\{Cu(apox)\}]^{2+}$ dinuclear species is known where L′ represents a polydentate outer ligand coordinated to M [33,43–50]. The structural characterization of some of them such as those of formula $[Ni(phen)_2Cu(apox)](ClO_4)_2 \cdot CH_3OH$ (phen > 1,10-phenanthroline) [44] and $[Mn(cth)Cu(apox)](CF_3SO_3)_2$ (cth = (±)-5,7,7,12,14,14-hexamethyl-1,4,8,11-tetraazacyclotetradecane) [50] shows once more that the *cis* conformation of apox is preserved.

In the light of these solution and solid state studies, it can be concluded that the apox ligand always exhibits the *cis* conformation in the Cu(apox)-containing heteropolymetallic species (step c in Scheme 7). Nevertheless, this conformation can be observed also in dinuclear copper(II) complexes provided that a suitable blocking ligand is previously bound to the second copper(II) ion. This is the case in the structure of the complex $[Cu(bipy)Cu(apox)](ClO_4)_2$ (bipy = 2,2′-bipyridine) (Fig. 9) [51] where the [Cu(apox] complex acts as a bidentate ligand towards the $[Cu(bipy)]^{2+}$ unit. Recently, it has been shown how the reaction of [Cu(apox)] and $[Cu_2(apox)]^{2+}$ as ligands towards $[Cu(bpm)]^{2+}$ and bpm (bpm = 2,2′-bipyrimidine), respectively, allows the preparation of three compounds of formula $[Cu(bpm)Cu(apox)](ClO_4)_2{\cdot}CH_3OH$, $[Cu_2(apox)(bpm)_2](ClO_4)_2{\cdot}2H_2O$ and $[Cu_2(apox)(bpm)](ClO_4)_2{\cdot}2H_2O$ [52]. The two first compounds are dimeric with apox adopting the *cis*- (first) and *trans-conformations* (second) and bpm acting as a terminal bidentate ligand (both compounds). The third example is an alternating copper(II) chain with a regular alternation of bis(terdentate) apox and bis(bidentate) bpm. This family of complexes illustrates how two simple tools such as the metal to oxamidate molar ratio and the coordinating properties of the coligand allow the synthetic chemist to design a great diversity of nuclearity tailored polynuclear species.

The *trans* conformation of the apox ligand is restricted to the homodinuclear species in the absence of any other ligand, the final complex being centrosymmetric (step a in Scheme 7). The *cis–trans* conformational change of apox in its metal complexes is responsible for the apparent anomalies in the trends of the computed stability constants (Fig. 10). As expected from the Irving–Williams series, the

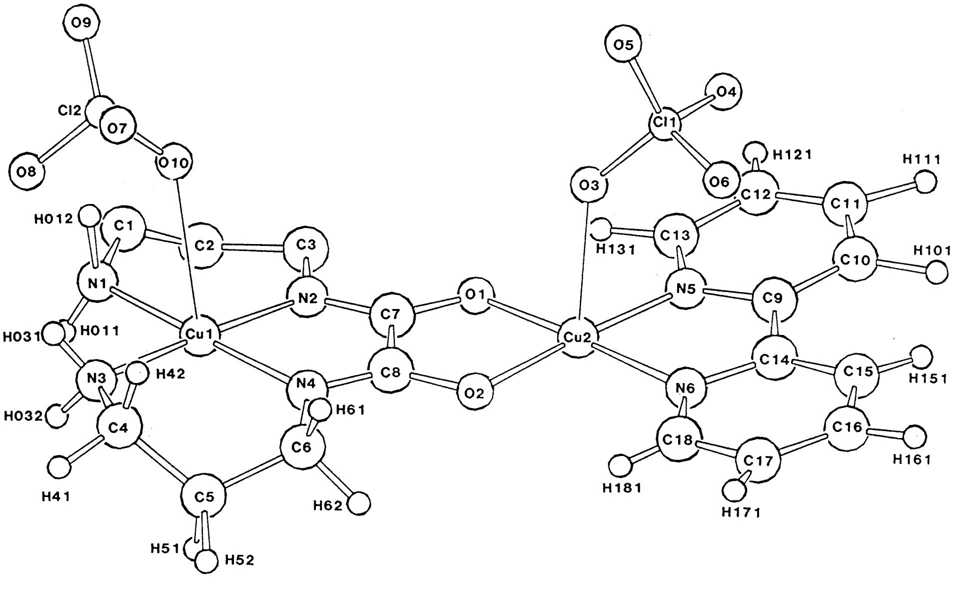

Fig. 9. Molecular structure of $[Cu(apox)Cu(bipy)(ClO_4)_2]$. (Reprinted with permission from Journaux et al. [51]. Copyright © 1985 American Chemical Society.)

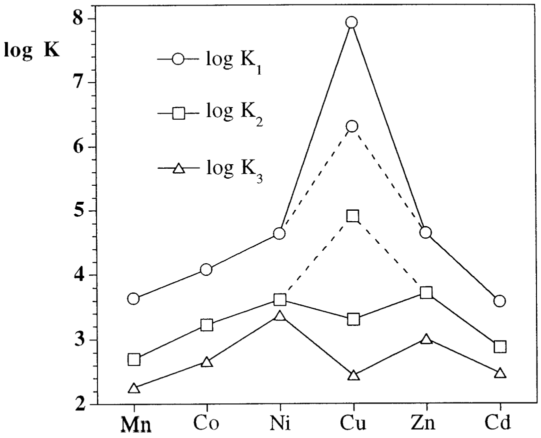

Fig. 10. Plot of the stepwise stability constants (log K_n, $n = 1-3$) for different metal ions.: experimental values (solid line); values calculated taking into account the conformational change (dashed line). (Reprinted with permission from Lloret et al. [21]. Copyright © 1992 American Chemical Society.)

values of the stability constants should increase when going from Mn(II) to Cu(II) and decrease for Zn(II) (or Cd(II)). However, the value of log K_1 (see Table 2) for Cu(II)–[Cu(apox)] is too high whereas that of log K_2 is too low (even lower than log K_2 for Ni(II)). The value of log K_3 is also very small, but this is as expected because of the Jahn–Teller effect accompanying the coordination of the third [Cu(apox)] unit. The anomalous values of log K_2 and log K_3 can be explained by taking into account the energetic cost of the oxamidate *cis–trans* conformational change. When 1 mmol of [Cu(apox)] reacts with 1 mmol of Cu(II), the *cis* conformation of apox in the mononuclear complex changes to the *trans* one in the corresponding copper(II) dimer (step a in Scheme 7), and this *trans* conformation moves the *cis* one by further coordination of a second [Cu(apox)] unit to afford the $[Cu_3(apox)_2]^{2+}$ trimer (step b in Scheme 7).

The higher stability of the *trans* conformer with regards to the *cis* one provides an additional stabilization of the dimeric species and consequently, a decrease of the stability of the trimeric one. No conformational change occurs in the complex formation between [Cu(apox) and M(II) (M $\neq$ Cu, steps c–e in Scheme 7). Assuming that the participation of copper(II) in Eq. (i) (Scheme 6a) does not significantly modify the value of the enthalpy of the system (i.e. $\Delta H' \sim \Delta H$ Eqs. (i) and (ii), Scheme 6a) and that $|\Delta S| < < |\Delta H|$, then $\Delta G \sim \Delta H$ (Eqn (ii)) and a value of log $K = 1.6$ is easily computed. So, considering this energetic cost of the *cis–trans* conformational change, the values of the equilibrium constants of Eq. (2) (log K'_1) and Eq. (3)

$$[Cu_2(apox)^{cis}] + Cu^{2+} \rightleftarrows [Cu_2(apox)^{cis}]^{2+};\ \log K'_1 = 7.9 - 1.6 = 6.3 \tag{2}$$

$$[Cu_2(apox)^{cis}]^{2+} + [Cu(apox)^{cis}] \rightleftarrows [Cu_3(apox)_2^{cis}]^{2+};\ \log K'_2 = 3.3 + 1.6 = 4.9 \tag{3}$$

($\log K'_2$) are easily calculated. These corrected values fit better the expected trend (dashed line in Fig. 10).

3.2. Influence of the size of the alkyl substituents in N,N′-bis(aminoalkyl)oxamidate copper(II) complexes

The modifications of the complexing ability of *N,N′*-substituted oxamides caused by the presence of alkyl substituents on their amino groups are exemplified well by the studies of complex formation between copper(II) and the ligands **2** and **3** [22]. The stoichiometries and stability constants of the observed species in solution for both systems are listed in Table 1. The corresponding distribution diagrams and the sequence of complex formation are shown in Fig. 11 and Scheme 9, respectively.

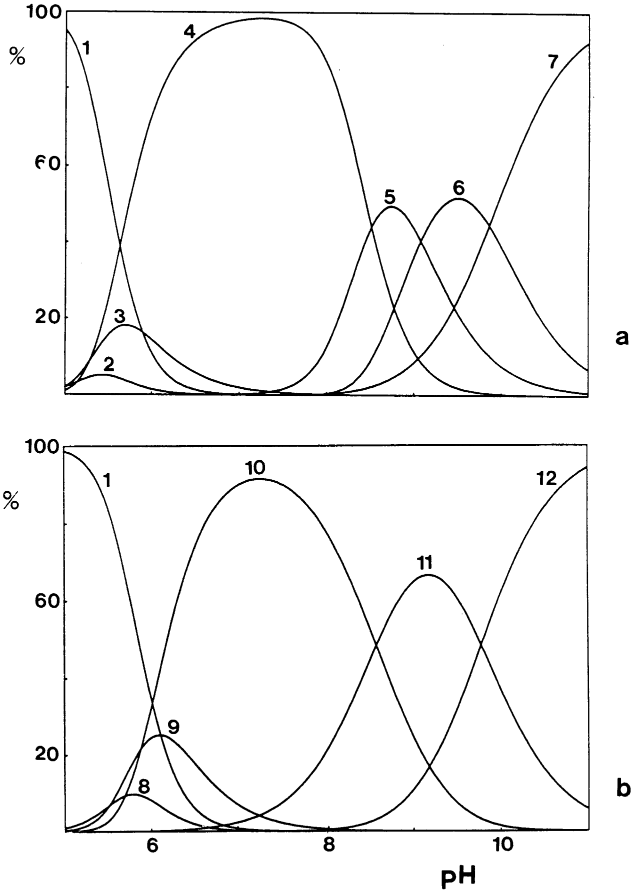

Fig. 11. Distribution diagrams for the system Cu^{2+}–L^{2-}–H^+ with L = mapox (a) and dmapox (b).($c_{Cu} = c_L = 5 \times 10^{-3}$ mol dm^{-3}). Complexes 1, 2, 3, 4, 5, 6, 7, 8 and 9 correspond to $[Cu^{2+}]$, $[Cu_2(H_2L)]^{4+}$, $[Cu_2(HL)]^{3+}$, $[Cu_2L]^{2+}$, $[Cu_3L_2]^{2+}$, $[Cu_4L_3]^{2+}$, [CuL], $[Cu_2L(OH)]^+$ and $[Cu_2L(OH)_2]$, respectively. (Reprinted with permission from Lloret et al. [22]. Copyright © 1992 American Chemical Society.)

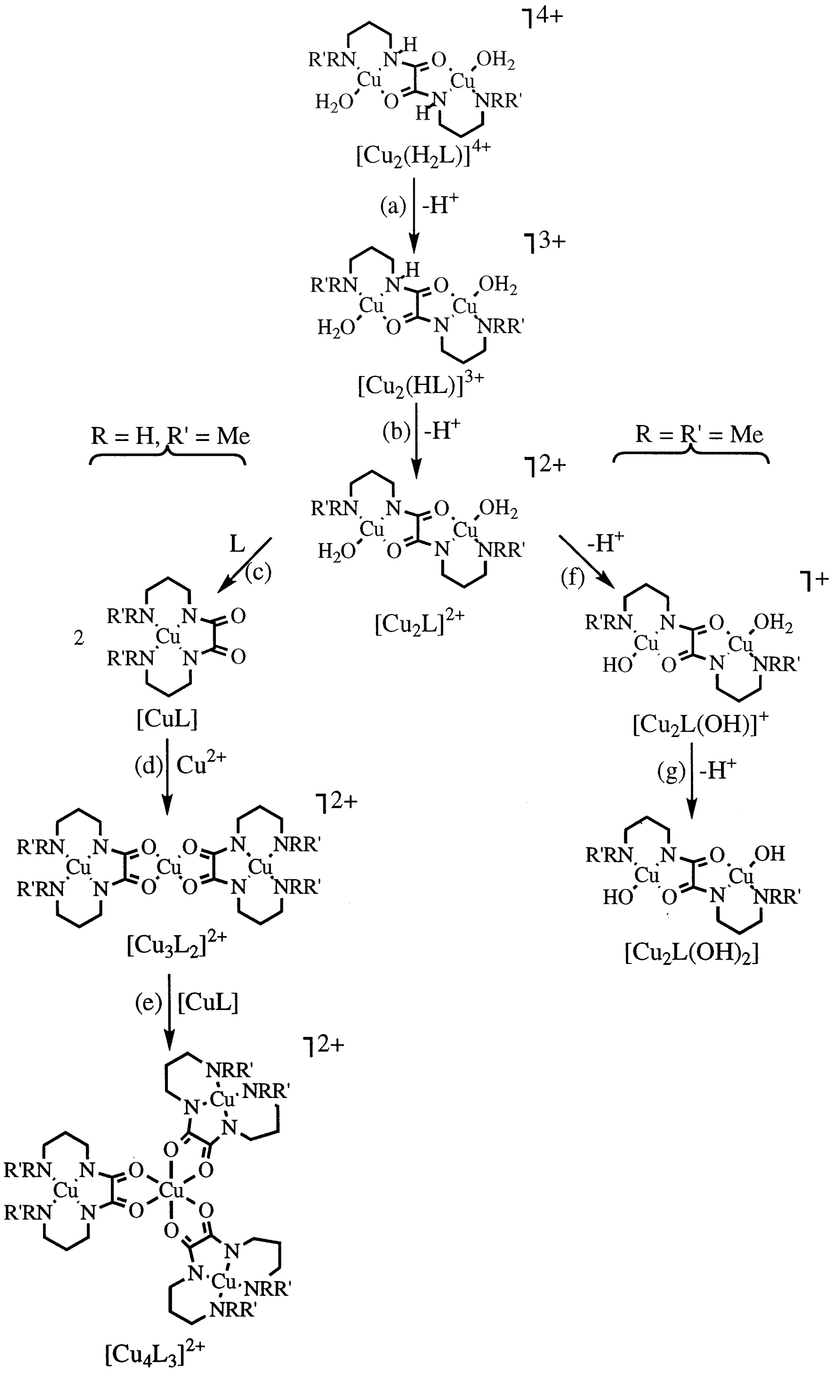
[Cu$_2$(H$_2$L)]$^{4+}$
(a) -H$^+$
[Cu$_2$(HL)]$^{3+}$
(b) -H$^+$
R = H, R' = Me
R = R' = Me
[Cu$_2$L]$^{2+}$
L (c)
2 [CuL]
(d) Cu^{2+}
[Cu$_3$L$_2$]$^{2+}$
(e) [CuL]
[Cu$_4$L$_3$]$^{2+}$
(f) -H$^+$
[Cu$_2$L(OH)]$^+$
(g) -H$^+$
[Cu$_2$L(OH)$_2$]

Scheme 9.

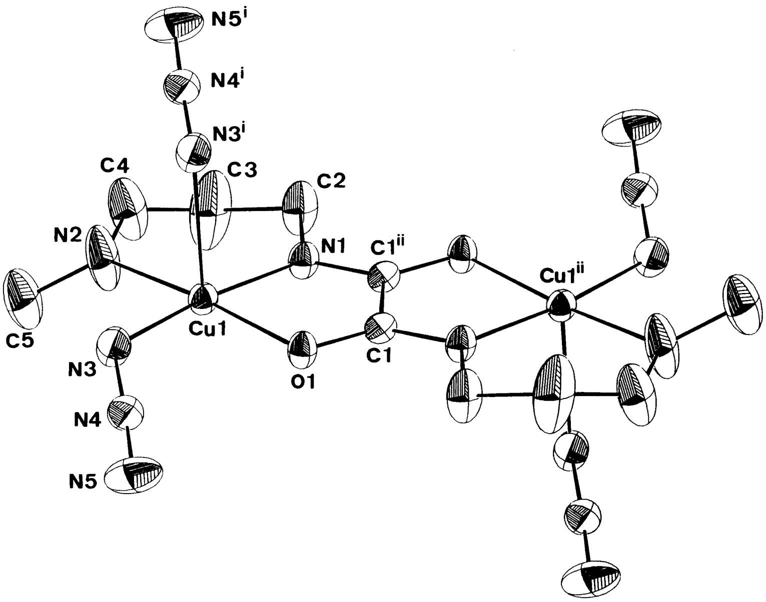

Fig. 12. Molecular structure of $[Cu_2(mapox)(N_3)_2]$. (Reprinted with permission from Lloret et al. [22]. Copyright © 1992 American Chemical Society.)

Both systems form similar complexes in the acidic region, the dinuclear $[Cu_2L]^{2+}$ (L = mapox and dmapox) complex being the main species in neutral conditions. Indeed, this species is readily isolated by adding bromide or pseudohalide (azide, cyanate or thiocyanate) as precipitating anions to aqueous solutions of $[Cu_2L]^{2+}$. These anions not only counterbalance the charge of the cation but also act as ligands, as illustrated by the structure of $[Cu_2(mapox)(N_3)_2]$ [22] (Fig. 12). The other $[Cu_2(H_2L)]^{4+}$ and $[Cu_2(HL)]^{3+}$ dinuclear species (step a in Scheme 9) only exist at lower pH values and they are minority species. Interestingly, both systems differ notably in the basic region. The mapox ligand is able to form the mononuclear copper(II) complex adopting the *cis* conformation, and thus the corresponding tri- and tetranuclear complexes (steps c–e, Scheme 9), as for the previous apox complexes. In contrast, the $[Cu(dmapox)^{cis}]$ monomer cannot exist because of the steric hindrance between the four amine–methyl groups (Scheme 10). In this case,

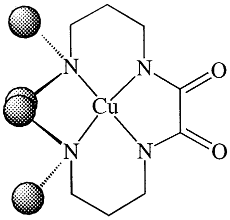

Scheme 10.

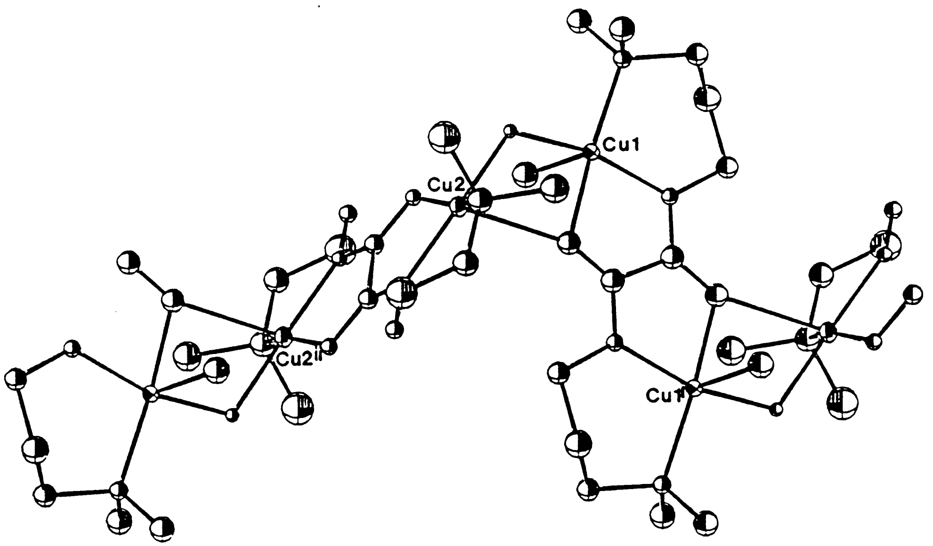

Fig. 13. Perspective drawing of a fragment of the alternating chain $[Cu_2(dmapox)(OH)(H_2O)]^+$.

the complex formation concerns the $[Cu_2(dmapox)]^{2+}$ dimer and the corresponding monohydroxo and dihydroxo species (steps f and g, Scheme 9) which are formed at high pH values. The deprotonation of the coordinated water molecules of the $[Cu_2(dmapox)]^{2+}$ complex affords these hydroxo species. Single crystals of the monohydroxo complex of formula $[Cu_2(dmapox)(OH)(H_2O)]NO_3$ (Fig. 13) were obtained by addition of sodium nitrate to aqueous solutions of $[Cu_2(dmapox)]^{2+}$ at pH ca. 9 [53]. Actually, this species is a copper(II) chain with regular alternation of hydroxo and oxamidato bridges which must be derived from the polymerization of the $[Cu_2(dmapox)(OH)]^+$ precursor (Scheme 11).

On the other hand, the trend of the values of the stepwise stability constants for the Cu^{2+}–$mapox^{2-}$ complexes (Eqs. (4)–(6)) ($\log K_1 = 9.32$, $\log K_2 = 3.78$ and $\log K_3 = 3.16$) [22]

$$[Cu(mapox)^{cis}] + Cu^{2+} \rightleftarrows [Cu_2(mapox)^{cis}]^{2+};\ \log K'_1 = 9.32 - 1.6 = 7.72 \qquad (4)$$

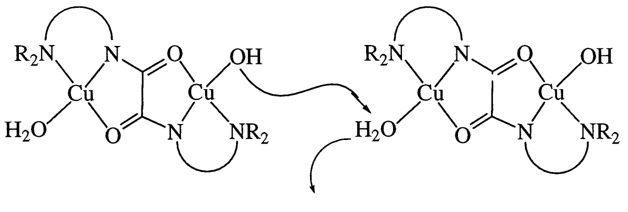

Scheme 11.

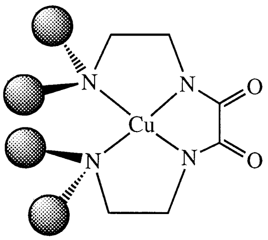

Scheme 12.

$$[\mathrm{Cu_2(mapox)}^{cis}]^{2+} + [\mathrm{Cu(mapox)}^{cis}] \rightleftarrows [\mathrm{Cu_3(mapox)}_2^{cis}]^{2+};\ \log K'_2 = 3.78 + 1.6 = 5.38 \qquad (5)$$

$$[\mathrm{Cu(mapox)}^{cis}] + [\mathrm{Cu_3(mapox)}_2^{cis}]^{2+} \rightleftarrows [\mathrm{Cu_4(mapox)}_3^{cis}]^{2+};\ \log K_3 = 3.16 \qquad (6)$$

reflects also the same anomaly observed in the Cu^{2+}–$apox^{2-}$ system because of the *cis–trans* conformational change (steps c–e, Scheme 9). This phenomenon is not observed for dmapox because the lack of the *cis* conformation for this ligand, the pattern of complex formation being different in that case(steps f and g, Scheme 9).

The steric hindrance is non-existent in the mononuclear [Cu(dmaeox)] (H_2dmaeox = *N*,*N'*-bis[2-(dimethylamino)ethyl]oxamide, **4**) (Scheme 12) due to the shortening of the alkyl arm ($n = 2$, Scheme 5). Consequently, the pattern of complex formation between Cu(II) and **4** (Scheme 13) is identical to that observed for **1** and **3** [23]. The $[Cu_2(dmaeox)]^{2+}$ dimer is the predominant species under neutral conditions in a wide pH range (Fig. 14) whereas the [Cu(dmaeox)] complex is the only existing one at pH ≥ 10.5. Significant amounts of the $[Cu_3(dmaeox)_2]^{2+}$

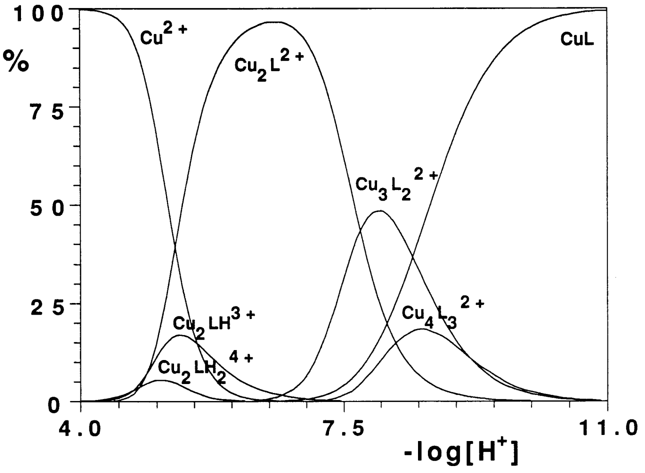

Fig. 14. Distribution diagram for the system Cu^{2+}–$dmaeox^{2-}$–H^+ as a function of pH ($c_{Cu} = c_L = 5 \times 10^{-3}$ mol dm^{-3}). (Reproduced with permission from Real et al. [23]. Copyright © 1993 The Royal Society of Chemistry.)

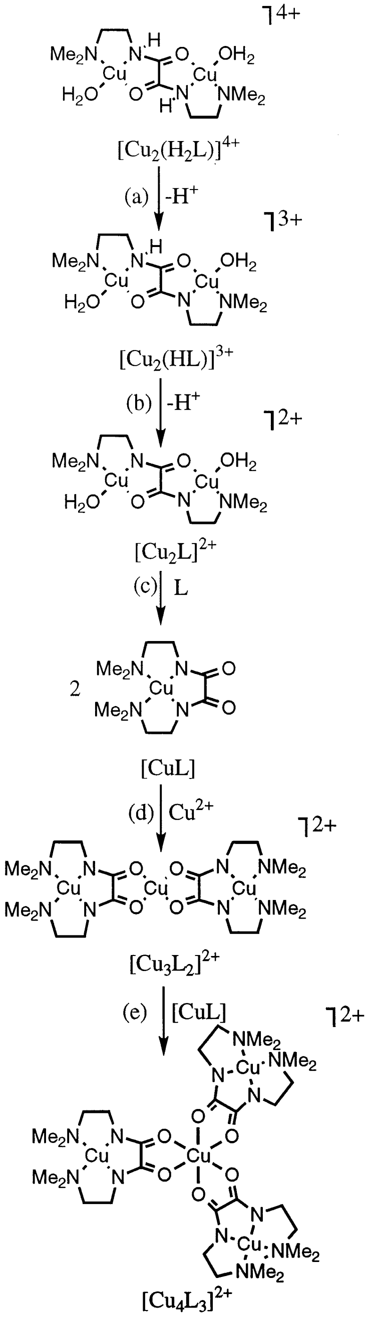
[Cu2(H2L)]4+
(a) -H+
[Cu2(HL)]3+
(b) -H+
[Cu2L]2+
(c) L
2
[CuL]
(d) Cu2+
[Cu3L2]2+
(e) [CuL]
[Cu4L3]2+
Me2N
NMe2
Cu
H2O
OH2
H
4+
3+
2+

Scheme 13.

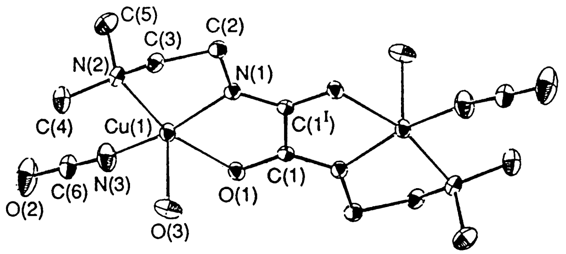

Fig. 15. Molecular structure of $[Cu_2(dmaeox)(NCO)_2(H_2O)_2]$. (Reproduced with permission from Real et al. [23]. Copyright © 1993 The Royal Society of Chemistry.)

tri- and $[Cu_4(dmaeox)_3]^{2+}$ tetranuclear complexes are present in the pH range 7.3–9.5.

The *trans* conformation of the dmaeox ligand is restricted to the $[Cu_2(dmaeox)]^{2+}$ unit as shown by the crystal structures of the complexes $[Cu_2(dmaeox)(NCO)_2(H_2O)_2]$ [23] (Fig. 15), $[Cu_2(dmaeox)(N_3)_2(H_2O)_2]$ (Fig. 16a) [54], $[Cu_2(dmaeox)(N_3)_2]$ (Fig. 16b) [54], and $[Cu_2(dmaeox)(NCS)_2(dmf)_2]$ (dmf = dimethylformamide) [55]. It is interesting to note that in the presence of azide, the $[Cu_2(dmaeox)]^{2+}$ unit can crystallize as a dimer with two axially bound water

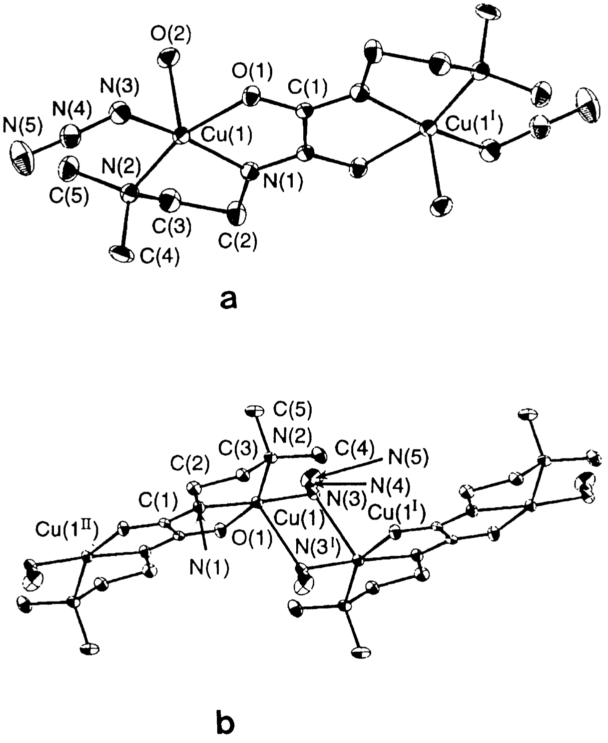

Fig. 16. Molecular structure of (a) $[Cu_2(dmaeox)(N_3)_2(H_2O)_2]$ and (b) $[Cu_2(dmaeox)(N_3)_2]$. (Reproduced with permission from Real et al. [54]. Copyright © 1994 The Royal Society of Chemistry.)

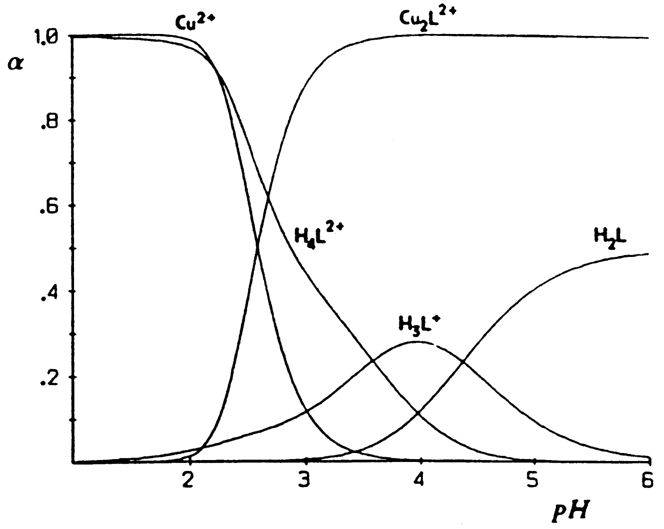

Fig. 17. Distribution diagram for the system Cu^{2+}–$pmox^{2-}$–H^+ as a function of pH ($c_{Cu} = c_L = 5 \times 10^{-3}$ mol dm^{-3}). (Reprinted with permission from Lloret et al. [19]. Copyright © 1989 American Chemical Society.)

molecules (Fig. 16a) as well as a polymer where the water molecules are replaced by azido groups adopting the μ-1,1-bridging mode.

The high value of the overall stability constant of $[Cu_2(dmaeox)]^{2+}$ ($\log \beta_{21} > 24.7$, Table 1) is consistent with the bis(terdentate) character of the dmaeox ligand, but it is ca. four orders of magnitude smaller than that reported for the parent $[Cu_2(apox)]^{2+}$ ($\log \beta_{21} = 28.1$, Table 1). The occurrence of alternating six- and five-membered fused chelates in the latter versus five-membered ones in the former, accounts for the greater stability of the apox dimer. The same situation is observed when comparing the values of the overall stability constants of the mononuclear [Cu(dmaeox)] ($\log \beta_{11} = 16.9$) and [Cu(apox)] ($\log \beta_{11} = 20.2$) complexes where 5–5–5 (dmaeox) and 6–5–6 (apox) membered fused chelates are involved.

As in preceding examples, the corrected values of the stepwise stability constants (assuming that the *cis–trans* conformational change of **1** is identical to that of **4**) fit better the expected trend from a purely statistical viewpoint (Eqs. (7)–(9)).

$$[Cu(dmaeox)^{cis}] + Cu^{2+} \rightleftarrows [Cu_2(dmaeox)^{cis}]^{2+};\ \log K'_1 = 7.82 - 1.6 = 6.22 \tag{7}$$

$$[Cu_2(dmaeox)^{cis}]^{2+} + [Cu(dmaeox)^{cis}] \rightleftarrows [Cu_3(dmaeox)_2^{cis}]^{2+};\ \log K'_2 = 3.21 + 1.6 = 4.81 \tag{8}$$

$$[Cu(dmaeox)^{cis}] + [Cu_3(dmaeox)_2^{cis}]^{2+} \rightleftarrows [Cu_4(dmaeox)_3^{cis}]^{2+};\ \log K_3 = 2.30 \tag{9}$$

The solution studies of complex formation between Cu(II) and H_2pmox (**6**) [19] deserve special mention . The $[Cu_2(pmox)]^{2+}$ dimer is a very stable species ($\log \beta_{21} = 26.1$, Table 1) Its formation in aqueous solution occurs in the pH range

2.0–3.5 and it is the only existing copper(II) complex at pH ≥ 3.5 (Fig. 17). The lower basicity of the pendant pyridyl group with respect to that of the amine makes possible the coexistence of the $[Cu_2(pmox)]^{2+}$ dimer and significant amounts of the free neutral ligand. The subsequent replacement of coordinated water molecules of the $[Cu_2(pmox)]^{2+}$ species by the pyridyl groups of **6** affords the alternating copper(II) chain of formula $[Cu_2(pmox)(H_2pmox)(H_2O)_2](NO_3)_2 \cdot 8H_2O$ [19], where regular alternation of bis(terdentate) $pmox^{2-}$ and *trans* bis(monodentate) H_2pmox occurs (Fig. 18).

Higher pH values could not be investigated in aqueous solution because the precipitation of this compound. However, it redissolves by increasing the pH and the [Cu(pmox)] mononuclear complex can be isolated from these solutions as a violet powder [56]. All our attempts to prepare the parent mononuclear copper(II) complex with H_2peox (**7**) were unsuccessful, most likely due to the steric hindrance between the two pyridyl rings of peox ligand in the *cis* conformation. To the best of our knowledge, only the *trans* conformation of the peox ligand has been structurally characterized as in the complex $[Cu_2(peox)(H_2O)_2(ClO_4)_2] \cdot 2H_2O$ (Fig. 19) [57].

3.3. *N,N′-bis(carboxyalkyl)oxamidate complexes*

The coordination chemistry of this type of oxamidate ligands such as **8** and **9** differs considerably from that of **1**–**6**. Basically, the differences are caused by (a) the different charge of the oxamidate ligand and (b) the versatility of the carboxylate group as ligand. The full deprotonation of these carboxylate–oxamidate ligands leads to L^{4-} tetraanionic species which can form the $[CuL]^{2-}$ mononuclear and $[Cu_2L]$ dinuclear species when adopting the *cis*- and t*rans*-conformations,

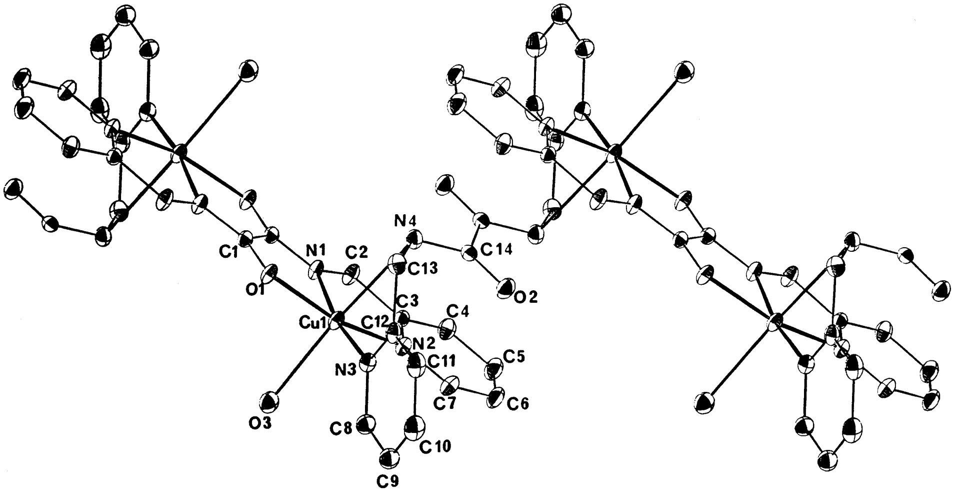

Fig. 18. Perspective drawing of a fragment of the alternating chain $[Cu_2(pmox)(H_2pmox)(H_2O)_2]^{2+}$. (Reprinted with permission from Lloret et al. [19]. Copyright © 1989 American Chemical Society.)

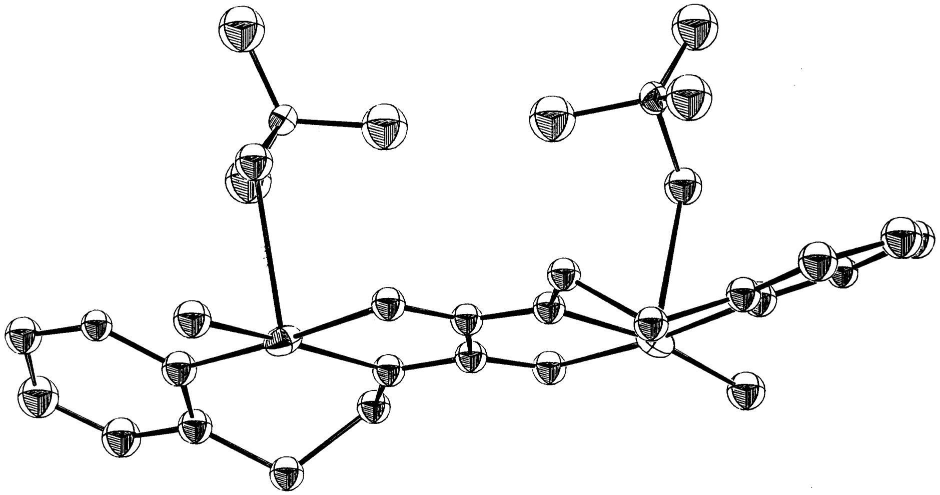

Fig. 19. Molecular structure of $[Cu_2(peox)(H_2O)_2(ClO_4)_2]$.

respectively. The oxamidato-bridged dimers would be neutral species scarcely soluble in polar solvents such as water. Their low solubility would preclude the formation of higher nuclearity species. Thus, the investigation of the complex formation with this kind of ligands in aqueous solution is difficult because the precipitation during the titration process.

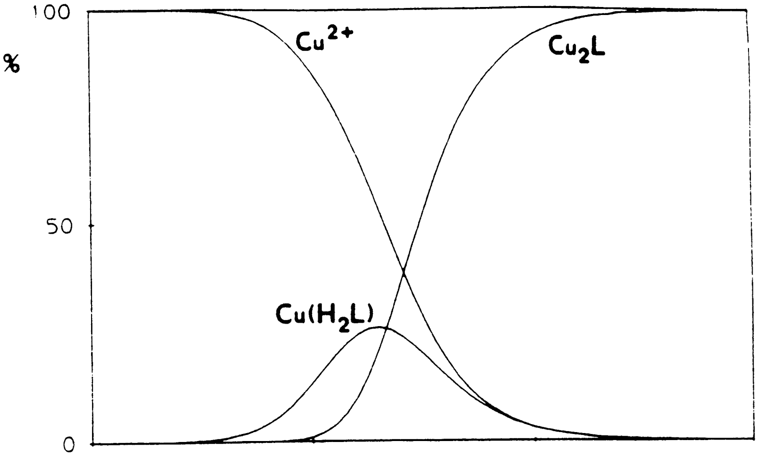

Fig. 20. Distribution diagram for the system Cu^{2+}–$glyox^{4-}$–H^+ as a function of pH ($c_{Cu} = c_L = 5 \times 10^{-3}$ mol dm^{-3}). (Reprinted with permission from Lloret et al. [20]. Copyright © 1992 American Chemical Society.)

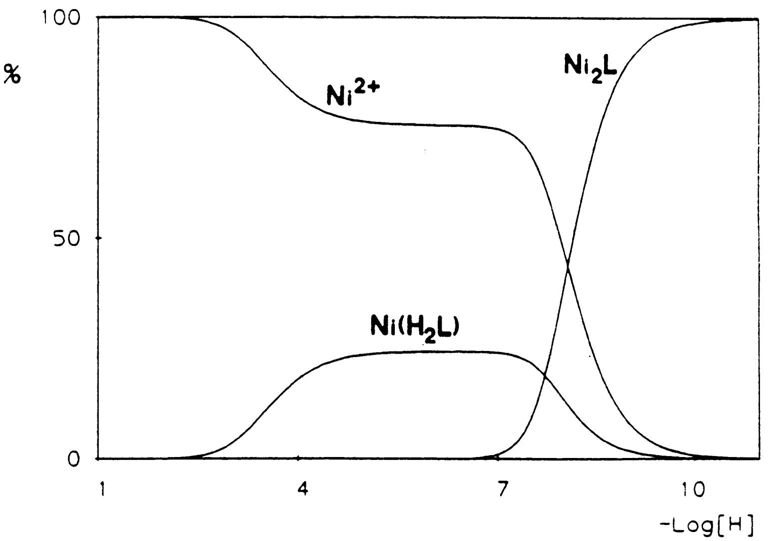

Fig. 21. Distribution diagram for the system Ni^{2+}–$glyox^{4-}$–H^{+} as a function of pH ($c_{Ni} = c_L = 5 \times 10^{-3}$ mol dm^{-3}). (Reprinted with permission from Lloret et al. [20]. Copyright © 1992 American Chemical Society.)

The study of complex formation between **8** and M(II) (M = Cu, Ni) (Figs. 20 and 21) [20] shows that significant amounts of [$M(H_2glyox)$] (M = Cu(II) and Ni(II)) are formed in the acidic region, whereas the neutral [$M_2(glyox)$] complex becomes the main species at pH values greater than 4 (Cu(II)) and 8 (Ni(II)). However, the precipitation of this complex at pH ≥ 5 (Cu(II)) and ≥ 9 (Ni(II)) precludes formation of higher species and makes impossible the potentiometric study at greater pH values. The [$M_2(glyox)$] species is readily soluble in more basic media and the resulting $[M(glyox)]^{2-}$ mononuclear compound can be isolated as a sodium salt of formula $Na_2[M(glyox)] \cdot nH_2O$ with $n = 4$ (Cu, blue) and 5 (Ni, green).

The knowledge of the existing species in solution provides the synthetic chemist with a precious information for preparative purposes. In the present case, single crystals of the $[Cu(H_2glyox)(H_2O)_3] \cdot 4H_2O$ chain compound (Fig. 22) and the $[Ni_2(glyox)(H_2O)_6] \cdot 4H_2O$ (Fig. 23) were obtained by slow evaporation of aqueous

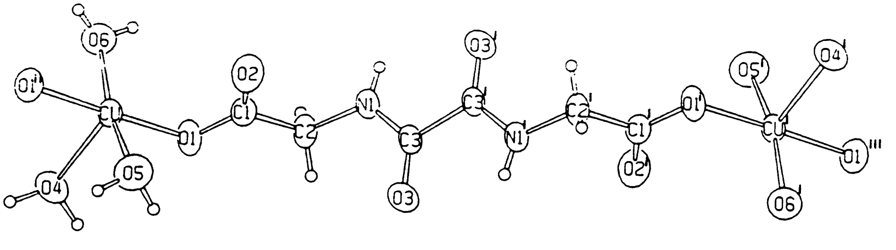

Fig. 22. Perspective drawing of a fragment of the copper(II) chain $[Cu(H_2glyox)(H_2O)_3] \cdot 4H_2O$. (Reprinted with permission from Lloret et al. [20]. Copyright © 1992 American Chemical Society.)

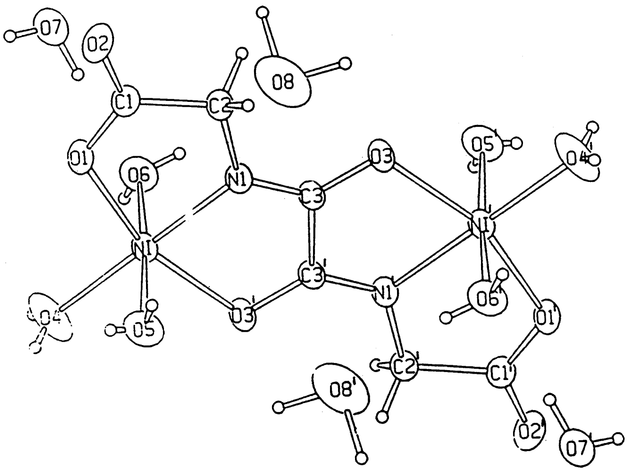

Fig. 23. Molecular structure of $[Ni_2(glyox)(H_2O)_6]\cdot 2H_2O$. (Reprinted with permission from Lloret et al. [20]. Copyright © 1992 American Chemical Society.)

solutions of **8** and Cu(II) or Ni(II) at pH ca. 3 and 7, respectively. The copper compound is formed through polymerization of the $[Cu(H_2glyox)]$ mononuclear species in a similar process to that illustrated by Scheme 11. The values of the stability constants of the $[M(H_2glyox)]$ complexes (Eq. (10)) are of the same

$$M^{2+} + H_2glyox^{2-} \rightleftarrows [M(H_2glyox)];\ \log K_1 = 2.62\ (Cu)\ \text{and}\ 1.93\ (Ni) \qquad (10)$$

order of magnitude that those for 1:1 M(II): carboxylate complexes where the carboxylate act as a monodentate ligand [58]. Therefore, H_2glyox^{2-} most likely coordinates to Cu(II) and Ni(II) through one of its carboxylate groups to yield the $[M(H_2glyox)]$ mononuclear species. The low value of $\log K_1$ in Eq. (10) ($\log K_1 > 3$) excludes a chelating behaviour in contrast to what it is observed in the $[Cu_2(H_2L)]$ copper(II) complexes with $H_2L = \mathbf{2}$ and **3** (Scheme 9) where the high value of the logarithm of the corresponding equilibrium constant (> 10, Table 1) supports it. As far as the $[M_2(glyox)]$ dimer is concerned, the high value of the stability constant (Eq. (11)) reveals the chelating character of the $glyox^{4-}$ ligand (Fig. 23). The loss of stability of

$$2M^{2+} + glyox^{4-} \rightleftarrows [M_2(glyox)];\ \log K_2 = 22.0\ (Cu)\ \text{and}\ 13.1\ (Ni) \qquad (11)$$

nine orders of magnitude of the dimer when copper(II) is replaced by Ni(II) illustrates once more the great selectivity of these oxamidate ligands towards copper(II). It can be reasonably assumed that other divalent metal ions would form less stable oxamidate complexes and thus, their formation occurring at more basic media, would be prevented by the precipitation of insoluble metal hydroxides.

In an early solution study of complex formation between **9** and M(II) (M = Cu and Ni) in water [59], only a narrow pH range could be explored because of the precipitation of the neutral $[Cu_2(alanox)]$ dimer at $pH > 4.5$ and the slow formation of an hydroxilated colloid nickel(II)–oxamidate species at $pH > 10$. In this report, the equilibrium constants of Eqs. (12)–(14) were determined.

$$H_4alanox \rightleftarrows H^+ + H_3alanox^-;\ pKa_1 = 3.9 \qquad (12)$$

$$H_3alanox^- \rightleftarrows H^+ + H_2alanox^{2-};\ pKa_2 = 4.7 \qquad (13)$$

$$2Cu^{2+} + H_4alanox \rightleftarrows 4H^+ + [Cu_2(alanox)];\ pK' = 10.6 \qquad (14)$$

From these results and assuming that the overall deprotonation constant $H_2alanox^{2-}$ (Eq. (15)) is identical to that of H_2glyox^{2-} (Table 1), the global stability constant of the $[Cu_2(alanox)]$ complex can be easily calculated (log $\beta_{21} >$ 22.2). This value is very close to that of the parent

$$H_2alanox^{2-} \rightleftarrows 2H^+ + alanox^{4-};\ pK = pKa_3 + pKa_4 + 24.2 \qquad (15)$$

$[Cu_2(glyox)]$ supporting the bis(terdentate) coordination mode of alanox towards the copper atom. A comparison between the logarithms of the stability constants of the $[Cu_2(apox)]^{2+}$ and $[Cu_2(alanox)]$ (28.1 and 22.2, respectively) illustrates the stability effect derived from the higher basicity of the amine (apox) versus carboxylate (alanox) groups.

In general, oxamidate-containing nickel(II) complexes are diamagnetic (square planar nickel(II)) due to the coordination of the strong field amidate-nitrogens [36–39]. This is an undesired situation in magnetic studies. However, the structure of $[Ni_2(glyox)(H_2O)_6]\cdot 4H_2O$ (Fig. 23) reveals that paramagnetic oxamidate-bridged nickel(II) species can be obtained provided that the strength of the ligand field of the substituted oxamidate is decreased. This is done in the present example by choosing the appropriate X group (carboxylate instead of amine or pyrydyl, for instance) and introducing some angular strain (series of alternating five-membered chelate rings instead of alternating six- and five-membered ones). Along this line, $Na_2[Ni(glyox)]\cdot 5H_2O$ is a paramagnetic complex whereas $Na_2[Ni(alanox)]\cdot 3H_2O$ is a diamagnetic species [60]. The corresponding mononuclear copper(II) complexes have also been prepared. These mononuclear copper(II) complexes can acts as chelating ligands towards transition metal ions yielding heterodinuclear species such as $[NiCu(obbz)(H_2O)_4]\cdot 2H_2O$ [61] (Fig. 24) where obbz is the deprotonated form of **10** (see Scheme 16).

In addition, the ability of the carboxylate to act as bridging ligand would lead to alternating bimetallic chains with regular alternation of oxamidate and carboxylate bridges [61–63]. Examples of this kind of chains with obbz are the compounds $MnCu(obbz)\cdot 5H_2O$ [61] and $[MnCu(obbz)(H_2O)_3]\cdot dmf$ [63] (Fig. 25). Under partial desolvatation, these chains transform into the monohydrated species of formula $MnCu(obbz)\cdot H_2O$ which behaves as a molecular-based magnet with $T_c = 14$ K [61,63].

4. Metal complexes with polyoxamides

4.1. Bisoxamidato complexes

As indicated in Scheme 3d, bisoxamides can be prepared by reaction of diamines with ethyl oxalyl chloride. In general, these bisoxamides are scarcely soluble in water as well as in other common solvents, and thus the corresponding solution studies are difficult. However, they dissolve readily in basic methanolic solutions in the presence of copper(II) because the formation of the mononuclear complexes shown in Scheme 14a. These metal complexes can be isolated as tetraalkylammonium or tetraphenylphosphonium salts in a good yield. When R = R′ = H (Scheme 14a), the corresponding oxamato complexes (Scheme 14b) are formed through copper(II)-assisted hydrolysis of the primary amide in aqueous solution. The bisoxamidato copper(II) complexes can act as bisbidentate ligands towards other metal ions yielding bimetallic chains (Scheme 14c) or even two-dimensional honeycomb compounds (Fig. 26) [64,65]. The main interest of these bimetallic layered compounds lies in their magnetic properties. They present ferrimagnetic ordering at low temperatures [64] and large coercive magnetic fields [66].

4.2. Trisoxamidato complexes: a unusual trisoxamide cryptand

The reaction between *N*,*N*,*N*-tris(ethyloxamate-2-ethyl)amine (trenest) and *N*,*N*,*N*-tris(2-aminoethyl)amine (Scheme 3f) affords the cyclic criptand 1,4,7,10,13,16,21,24-octaazabicyclo[8.8.8]hexacosan-5,6,14,15,22,23-hexone (H_6L, **11**) in a high yield [67]. Its crystal structure (Fig. 27) reveals the occurrence of two

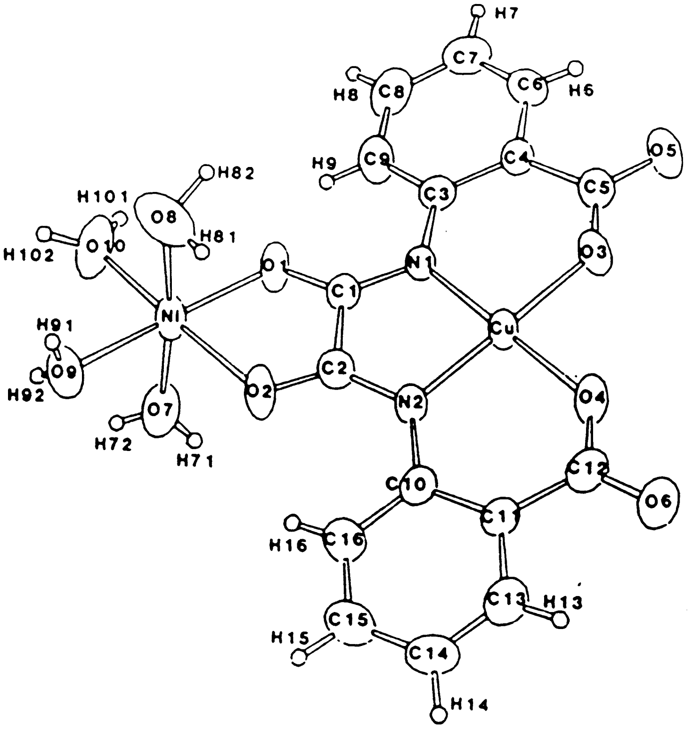

Fig. 24. Molecular structure of $[NiCu(obbz)(H_2O)_4]\cdot 2H_2O$. (Reprinted with permission from Nakatani et al. [61]. Copyright © American Chemical Society.)

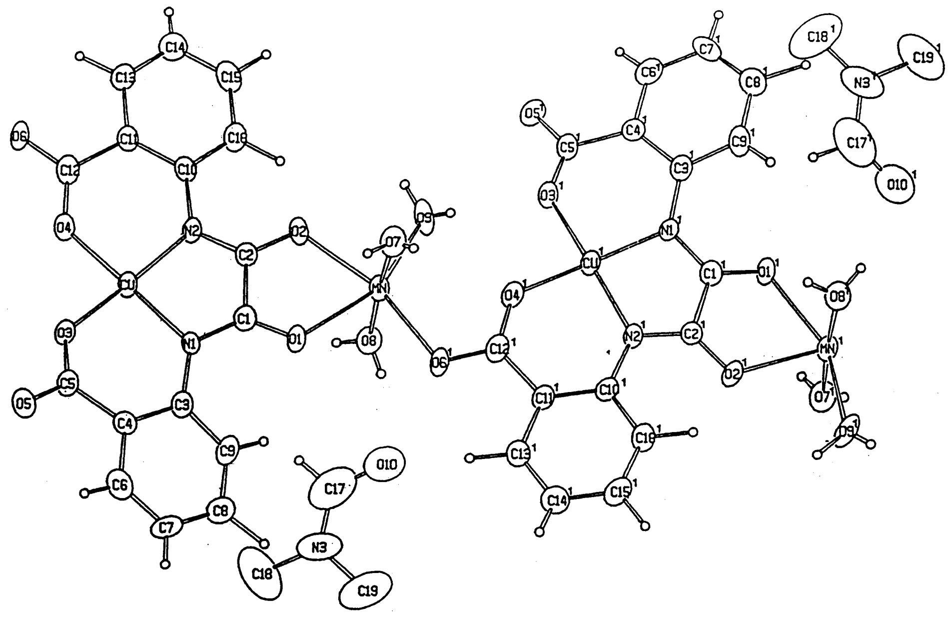

Fig. 25. Perspective drawing of a fragment of the alternating bimetallic chain $[MnCu(obbz)(H_2O)_3]{\cdot}dmf$. (Reprinted with permission from Lloret et al. [63]. Copyright © 1993 American Chemical Society.)

tertiary amino groups in an *endo–endo* conformation which are linked by three identical *N*,*N*′-bis(ethyl)oxamide branches. The protonation of **11** and its complex formation with Cu(II) was investigated by potentiometry in water and in a dmso–water (80:20 w/w) mixture as solvents. The stoichiometries of the existing species in solution and the corresponding equilibrium constants are listed in Table 4. As shown in this table, **11** behaves as a bis–base with $pKa_1 = 1.9$ and $pKa_2 = 7.1$ in water and $pKa_1 = 1.8$ and $pKa_2 = 6.75$ in dmso/H_2O. The striking large difference between pKa_1 and pKa_2 (ΔpK ca. 5) and the lower basicity of the N-bridgehead of **11** with respect to that of the model compounds trenest and trenox were attributed to cooperative phenomena in the cryptand. An inward rotation of the oxamide groups to form hydrogen bonds accompanies the protonation process of **11** accounts for this cooperativity (Fig. 28). Molecular mechanical calculations [68] performed on **11** and its protonated forms led to minima of energy with the oxamide group in *trans* conformation. Nevertheless, they can adopt different orientations with respect to the cavity as a function of the degree of protonation. For **11**, the calculations predict the form observed in the solid state (bridgehead lone pairs in *endo–endo* conformation and oxamide groups tangent to the cavity (Fig. 28a) as more stable). The impossibility of alkylation of **11** is chemically supports the occurrence of this *endo–endo* conformation. It is clear that hydrogen bonding between HN–amide and N–amine bridgehead are precluded in this conformation. The addition of the first proton to yield H_7L^+ causes the twisting inward of three of the carbonyl groups of the amide, forming three hydrogen bonds

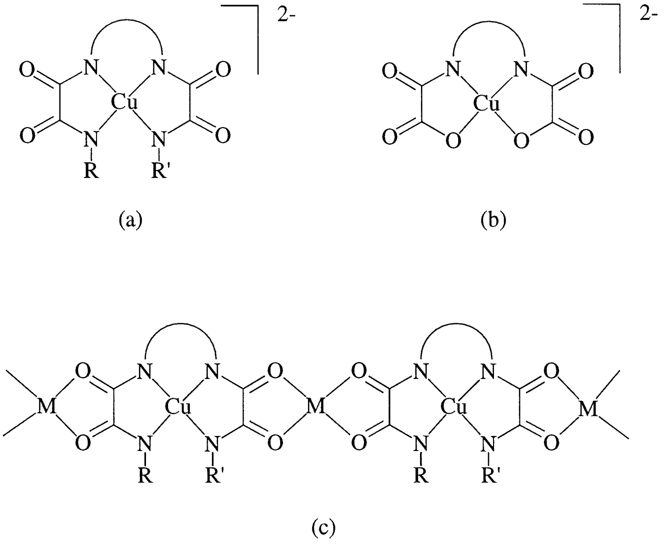

(a) (b)

(c)

Scheme 14.

with the *endo* H–N$^+$ and the other three hydrogen bonds between the remaining *endo* bridgehead amine group and the H–N amide (Fig. 28b). Such a conformation increases the electron density on one side of the cavity (enhancing thus its basicity)

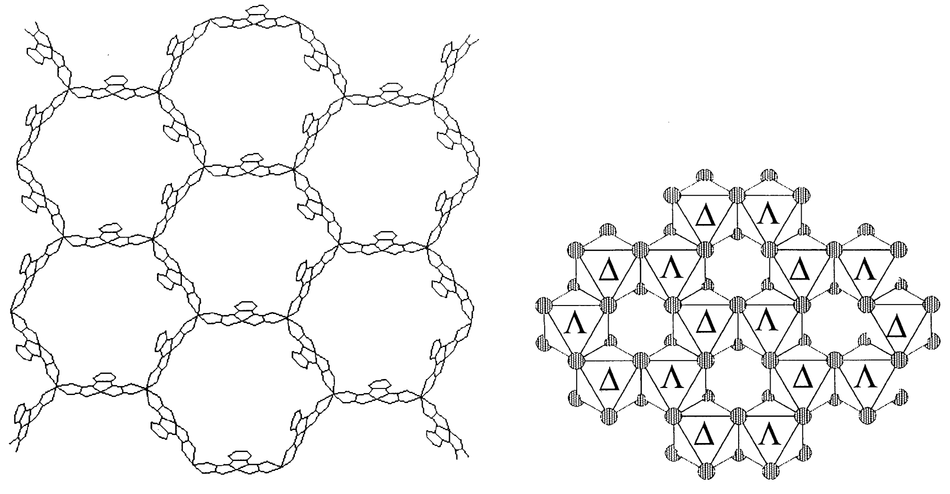

(a) (b)

Fig. 26. Suggested structure of (a) the anionic two-dimensional honeycomb $[M_2(CuL)_3]^{2-}$ (M = Mn(II), Fe(II), Co(II), Ni(II), Zn(II) and Cd(II)) and (b) view of the alternating enantiomers within the layer.

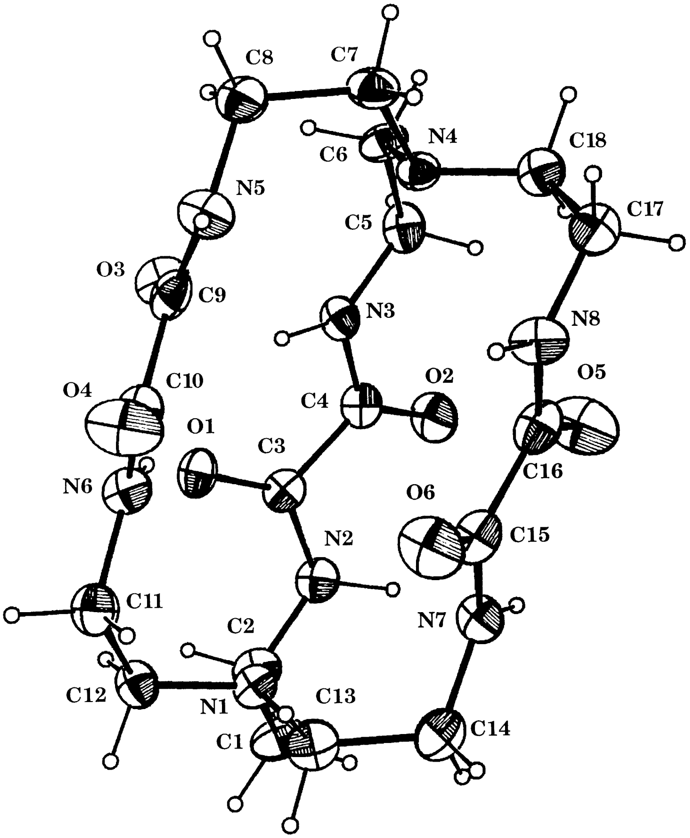

Fig. 27. Molecular structure of **11**. (Reprinted with permission from Colin et al. [67]. Copyright © 1996 Elsevier.)

whereas it decreases it in the opposite side (lowering its basicity). Consequently, the first protonation to yield H_7L^+ is favoured whereas the second one to yield H_8L^{2+} is disfavoured. Finally, the second protonation to yield H_8L^{2+} leads to an energy minimum for the *exo–exo* conformation with the oxamide group lying tangent to the cavity as in **11**. The difficulty to form hydrogen bonds inside the cavity of H_8L^{2+} is at the origin of the adoption of the *exo–exo* conformation which is most likely stabilized through hydrogen bonding with protic solvents. It deserves to be outlined that although some polyoxacryptands possessing tertiary amines sites at the bridgehead position also display cooperative proton binding [69–71], the trend of the proton affinity in them is the opposite to that observed in **11**.

In addition to the great variety of dinuclear copper(II) complexes detected in solution in the Cu^{2+}–**11** system as a function of the pH (Fig. 29) [67], the most appealing feature of this investigation was the occurrence of the copper(II)-assisted hydrolysis of **11** to yield a new macrocyclic ligand (which was structurally characterized under the form of a copper(II) dimer (Fig. 30)) [72]. The subsequent steps of the deprotonation of the $Cu_2(H_6L)^{4+}$ complex are shown in Scheme 15. The important geometric distortions arising from the coordination of the third oxamide group to copper in the basic region, causes the partial hydrolysis of the cryptand and one of the oxamide group is transformed into oxalate. Additional data on oxamidatocopper(II) complexes have shown that this copper(II)-promoted hydrolytic reaction is favoured by increasing the distortion of coordinated oxamidate group [73].

5. Electrochemical behaviour of oxamidate-containing metal complexes

5.1. Copper(III) complexes with mono- and bis(disubstituted)oxamides

The coordination chemistry of high oxidation state metal complexes of middle (Cr, Mn, Fe) and late (Co, Ni, Cu) first-row transition-metal ions is an area of considerable importance, both by their biological significance as redox enzyme

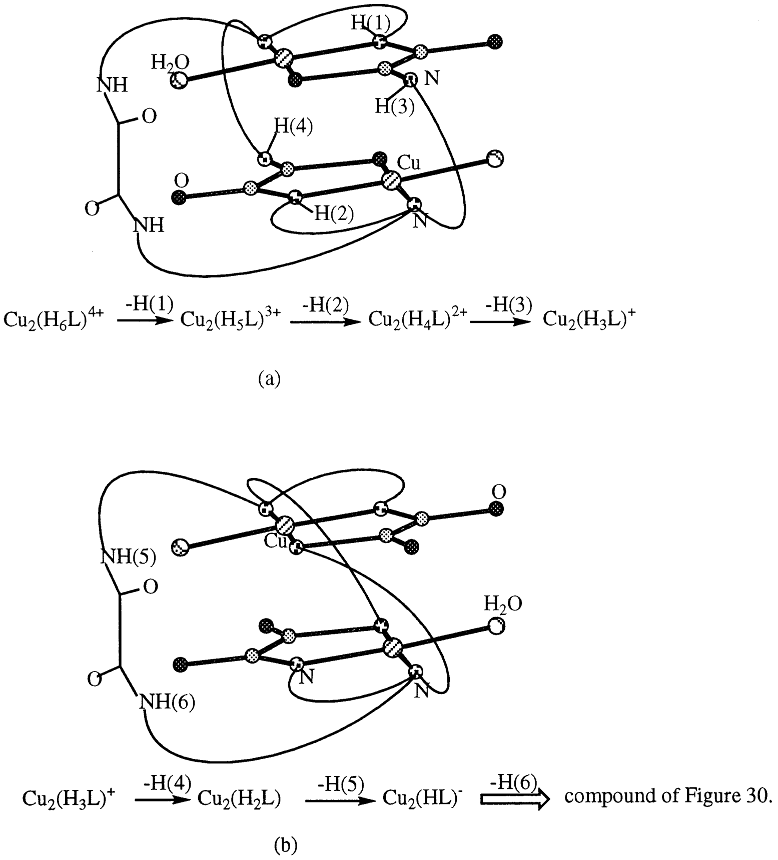

$$Cu_2(H_6L)^{4+} \xrightarrow{-H(1)} Cu_2(H_5L)^{3+} \xrightarrow{-H(2)} Cu_2(H_4L)^{2+} \xrightarrow{-H(3)} Cu_2(H_3L)^{+}$$

$$Cu_2(H_3L)^{+} \xrightarrow{-H(4)} Cu_2(H_2L) \xrightarrow{-H(5)} Cu_2(HL)^{-} \xRightarrow{-H(6)} \text{compound of Figure 30.}$$

Scheme 15.

models and potentially useful properties as catalytic oxidants. However, it is limited in scope due to the small number of suitable ligands [18,74,75]. The well known oxamide dianion, $C_2O_2N_2H_2^{2-}$, (Scheme 1) belongs to this family. The strong electron donating amidate nitrogen atoms are responsible for the occurrence of oxamidate-containing Cu(III) and Ni(III) complexes [14] but unfortunately, these high valent metal complexes are kinetically unstable and the coordinated oxamidate ligand undergoes a trivalent metal-assisted hydrolytic reaction yielding the oxalate and/or the corresponding oxalato complexes. These difficulties can almost be overcome by using *N*,*N*′-bis(coordinating group substituted)oxamides [15] which are more reluctant towards the hydrolysis. The possibility to stabilize the trivalent state of copper with these type of ligands was checked in two different solvents [73], the ligands used (Scheme 16) and the more relevant electrochemical data being summarized in Table 5. Linear sweep voltammetry of these compounds shows only one oxidation (A) in dmso. If the sweep is reversed after peak A, the corresponding reduction peak (A′) is detected for this series of complexes except for the iodo one, where it is not observed under our experimental conditions. The A/A′ couple appears to be not totally reversible for the remaining complexes, as indicated by the value of the $i_p(A)/i_p(A')$ ratio. In water, these complexes show an oxidation process but no reduction peak is observed (even at high scan rates), revealing that a fast chemical reaction is coupled to the electrochemical process. Controlled potential electrolysis and coulometry for these compounds in both solvents showed that the final oxidation process occurs after passage of 1 F mol^{-1}.

Two important points deserve to be outlined from this electrochemical study: firstly, the relatively easy oxidation of the oxamidate copper(II) complexes to the corresponding copper(III) ones and secondly, the strong dependence of these oxidation potentials on the donor character of the substituent on the phenyl ring

Table 4
Equilibrium data for basicity and formation of Cu(II) complexes with H_6L (10) at 25°C in dmso/H_2O (80:20 w/w) (0.1 mol dm^{-3} $KClO_4$) and H_2O (0.1 mol dm^{-3} KNO_3)

Reaction	log *K* dmso/H_2O	H_2O
$H_6L + H^+ \rightleftarrows H_7L^+$	6.75	7.10
$H_6L + 2H^+ \rightleftarrows H_8L^+$	8.55	9.00
$H_6L + 2Cu^{2+} \rightleftarrows [Cu_2(H_6L)]^{4+}$	6.15	6.88
$H_6L + 2Cu^{2+} \rightleftarrows [Cu_2(H_5L)]^{3+} + H^+$	1.21	1.59
$H_6L + 2Cu^{2+} \rightleftarrows [Cu_2(H_4L)]^{2+} + 2H^+$	−3.82	−3.90
$H_6L + 2Cu^{2+} \rightleftarrows [Cu_2(H_3L)]^{+} + 3H^+$	−9.22	−9.71
$H_6L + 2Cu^{2+} \rightleftarrows [Cu_2(H_2L)] + 4H^+$	−14.82	−15.72
$H_6L + 2Cu^{2+} \rightleftarrows [Cu_2(HL)]^{-} + 5H^+$	−22.7	–
trenox + $H^+ \rightleftarrows$ Htrenox^{+}[a]	4.0	4.2
trenest + $H^+ \rightleftarrows$ Htrenest^{+}[a]	–	5.22

[a] Models for the first protonation of **11**. Trenox and Trenest are shown in Scheme 3e.

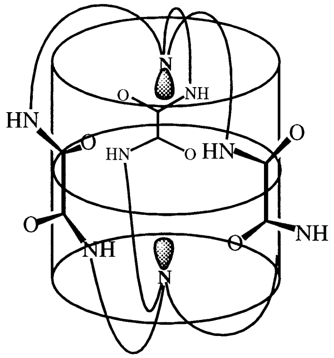

(a) H_6L (endo-endo)

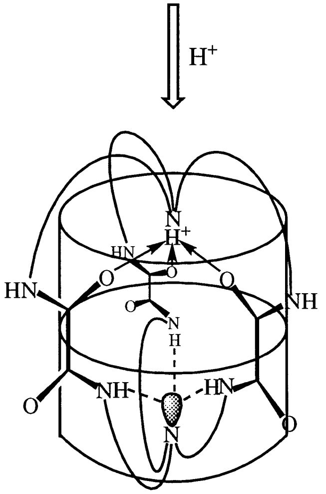

(b) H_7L^+ (endo-endo)

Fig. 28. Different orientations of the oxamide groups in **11** as a function of the protonation degree.

(obbz family). Concerning this latter point, the more electron donor the substituent is (MeO > Me > H > I > Br > Cl), the greater the basicity of the amide–N and carboxylate–O atoms are, leading to lower oxidation potentials. Along this line, the greater basicity of the aliphatic amide and carboxylate (compounds with obp and pba) with respect to the aromatic one (obbz family) leads to a significant decrease of the value of the oxidation potential, specially in dmso.

The oxamidate-containing copper(III) complexes are unstable species because of the copper(III)-catalyzed hydrolytic decomposition of the oxamidate ligand. The observed irreversibility in aqueous solution is due to this hydrolytic reaction. Its occurrence is supported by the lack of redox waves after the passage of 1 F per mol of complex in aqueous solution. Some reports have illustrated the capability of the copper(II) to promote the hydrolysis of primary amides in water yielding the corresponding carboxylates [5,11,12,36], and although secondary amides are more reluctant towards this process, they decompose slowly. So, it is not surprising that

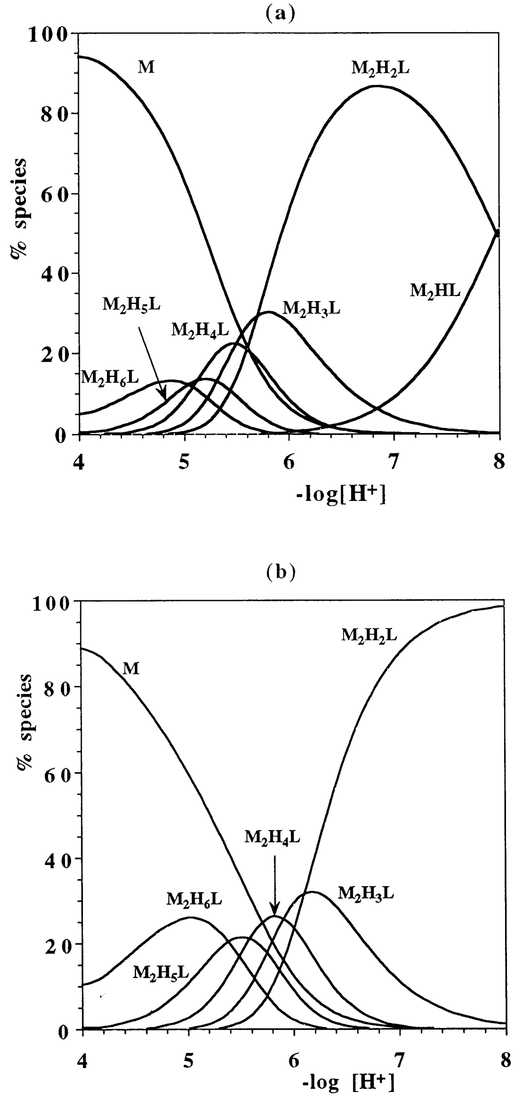

Fig. 29. Distribution diagram for the system Cu^{2+}–H_6L ($c_L = 2.5 \times 10^{-3}$ and $c_M = 5 \times 10^{-3}$ mol dm^{-3}) as a function of $-\log[H^+]$ in (a) dmso/water and (b) water. Charges are omitted for simplicity. The explored pH ranges are 3.5–7.5 (a) and 3.5–7.0 (b). (Reprinted with permission from Colin et al. [67]. Copyright © 1996 Elsevier.)

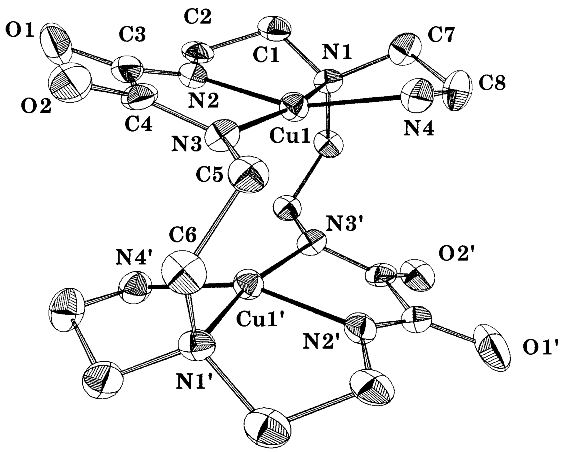

Fig. 30. Molecular structure of {1,10-bis(2-aminoethyl)-1,4,7,10,13,16-hexaazacycloocta-decane-5,6,14,15-tetronato(4-)}dicopper(II). (Reprinted with permission from Colin et al. [72]. Copyright © 1996 American Chemical Society.)

the stronger acidity of the copper(III) ion could catalyze easier this hydrolytic reaction. In the light of these features, it is clear that water as solvent has to be discarded in the preparation of oxamidatocopper(III) complexes. These species are more stable in dmso and their oxidation potentials are smaller and reversible in this solvent.

Finally, it is very interesting to point out that the oxidation of the iodo-derivative from Table 5 is totally irreversible in dmso. The structural knowledge of the complexes of formula $MnCu(obbz)(H_2O)_3 \cdot dmf$ [63], $MnCu(Cl_4obbz)(H_2O)_5$ [76] and $MnCu(Br_4obbz)(H_2O) \cdot 3.5H_2O$ [76] provides an explanation to this unexpected result. These structures show that the steric hindrance between the substituent in the three-position on the aromatic ring and the amide oxygen atom follows the trend $H > Cl > Br$, this trend being illustrated by the value of the dihedral angle α (Scheme 17) which decreases ($\alpha = 168.4$ (H), 145.2 (Cl) and 143.3° (Br)) as far as the steric repulsion increases. Although structural data for the iodo derivative are unknown, the value of a for this compound should be the smallest in the series. The value of the dihedral angle between the N(1)C(1)C(2)N(2) mean plane (noted A) and those of the aromatic rings (noted B and C) provides a better illustration of this feature: they are 18.1, 45.0 and 52.0° (between A and B) and 27.0, 53.0 and 58.6° (between A and C) for H, Cl and Br containing complexes, respectively. A greater bending is expected for the iodo derivative because of the larger radii of the iodine atom. The cleavage of the C(1)–N(1) and C(2)–N(2) bonds to yield the oxalate anion and the corresponding substituted 2-aminobenzoic acid as products is easier when the deviation from the planarity between the oxamidate skeleton and the phenyl rings is greater, most likely due to the increasing loss of electron density in the OCN oxamidate fragment.

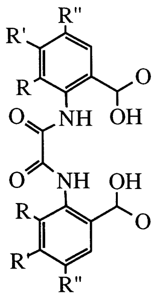

R = R' = R''= H (H_4obbz) (**10**)
R' = H, R = R'' = Cl (H_4Cl_4obbz) (**12**)
R' = H, R = R'' = Br (H_4Br_4obbz) (**13**)
R' = H, R = R'' = I (H_4I_4obbz) (**14**)
R = R' = H, R'' = Me (H_4Me_2obbz) (**15**)
R = H, R' = R'' =MeO ($H_4(MeO)_4$obbz) (**16**)

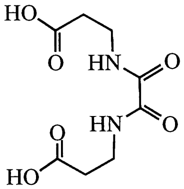

H_4alanox (**9**)

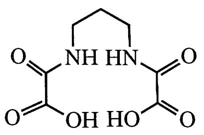

H_4pba (**17**)

Scheme 16.

This information is very important aiming at preparing oxamidatocopper(III) complexes. At this respect, the choice of substituted oxamides to generate more stable oxamidatocopper(III) species in solution and the search for adequate counterions to precipitate them have been the subject of recent works [77,78]. The results of the work carried out with a specific family of tetraanionic chelating *N,N'*-bis(aryl/alkyl-substituted)oxamide type ligands (**18**–**23**) in the stabilization of copper(III) complexes are summarized in Table 6. The trend in formal potentials of the copper(III)/copper(II) couples along the series opba > mopba > dmopba is ex-

Table 5
Electrochemical parameters for the Cu(III)/Cu(II) couple in monomeric Cu(II) complexes[a] in water and dmso at 25°C[b]

Compound	Solvent[c]H_2O $E_p(A)^{d,e}$	$E_p(A')^d$	dmso ΔE_p (mV)[f]
$Na_2[Cu(obbz)]$	0.92	0.76	96
$Na_2[Cu(Cl_4obbz)]$	1.19	0.86	126
$Na_2[Cu(Br_4obbz)]$	1.04	0.80	91
$Na_2[Cu(I_4obbz)]$	0.95	0.78	–
$Na_2[Cu(Me_2obbz)]$	1.00	0.68	101
$Na_2[Cu((MeO)_4obbz)]$	0.86	0.65	97
$Na_2[Cu(alanox)]$	0.92	0.51	82
$Na_2[Cu(pba)]$	0.97	0.55	98

[a] All data given at 100 mV s^{-1}.

[b] The ligands are defined in Scheme 16.

[c] 0.1 mol dm^{-3} $NaNO_3$ (H_2O) or n-Bu_4NPF_6 (dmso).

[d] Values referred to the saturated calomel electrode (SCE) using in all cases platinum as electrode.

[e] Values obtained at pH = 8.

[f] In the same conditions ferrocene gives an ΔE_p of 72 mV.

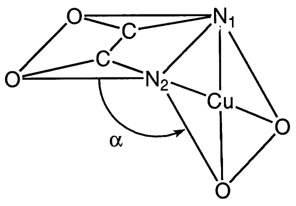

Scheme 17.

plained in terms of the stronger donor properties of the deprotonated-amide nitrogen atoms versus the carboxylate oxygen ones. Hence, the stabilization of trivalent oxidation state of copper is attributed to the increasing number of deprotonated amido donor groups.

It is interesting to note that the relative gain in the crystal field stabilization energy for the change from the d^9 (Cu(II), paramagnetic square planar) to the low-spin d^8 (Cu(III), diamagnetic square-planar) electronic configuration is the main factor in the overall thermodynamic stability of the copper(III) complex, as indicated by the perfect correlation between the Cu(III)/Cu(II) redox potential and the maximum of the visible absorption spectrum of the copper(II) complexes (Fig. 31).

Moreover, a significant electronic effect in the formal potential values is observed for the series dmopbaMe$_2$ > dmopba > dmopbaCl$_2$ > dmopba(NO$_2$)$_2$, as the ligands with electron-donating substituents into the benzene ring stabilize better the copper(III) oxidation state than those with electron-withdrawing ones. The stable

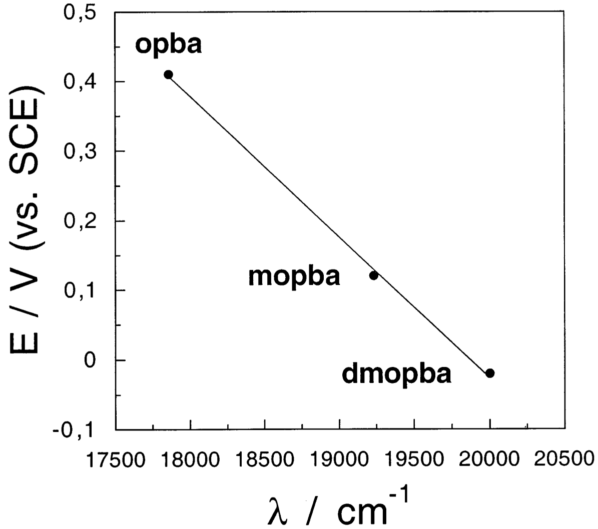

Fig. 31. Plot of the Cu(III)/Cu(II) redox potential as a function of the copper(II) d–d absorption maximum. (Reproduced with permission from Ruiz et al. [77]. Copyright © 1997 The Royal Society of Chemistry.)

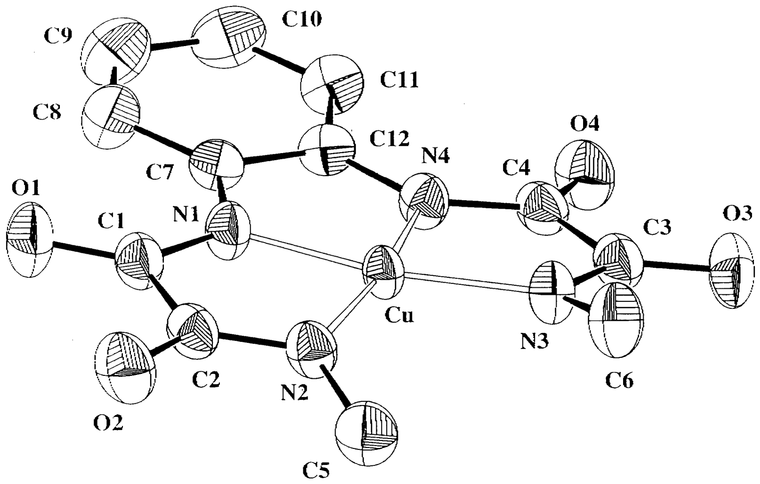

Fig. 32. Molecular structure of the copper(III) complex $[Cu(dmopba)]^-$. (Reproduced with permission from Ruiz et al. [77]. Copyright © 1997 The Royal Society of Chemistry.)

square-planar copper(III) complex of formula $PPh_4[Cu(dmopba)]\cdot MeCN$ (PPh_4^+ = tetraphenylphosphonium cation) (Fig. 32) [77] constitutes one of the few examples of structurally characterized copper(III) compounds [79–86]. These results on the coordination chemistry of oxamidato–copper(III) complexes complement the pioneering studies by Margerum (tri- and tetrapeptide complexes) [87,88], Fabbrizzi (cyclam and dioxocyclamato complexes) [89,90] and Collins (amidophenoxo and amidoalkoxo complexes) [81], which show that Cu(III) can no longer be considered a rare oxidation state.

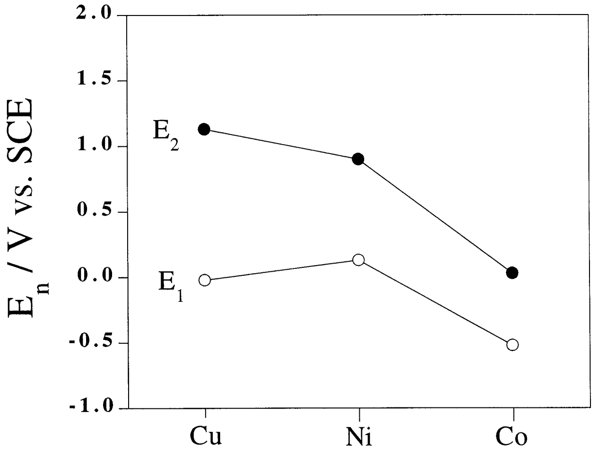

Fig. 33. Plot of the $[M(dmopba)]^-/[M(dmopba)]^{2-}$ (E_1) and $[M(dmopba)]/[M(dmopba)]^-$ (E_2) redox potentials (vs. SCE) against the metal ion (M = Cu, Ni and Co).

Table 6

Values of the Cu^{III}–Cu^{II} redox potentials for copper complexes of a related class of bis(disubstituted oxamido) ligands (acetonitrile, 25°C, 0.1 mol dm^{-3} NEt_4ClO_4)

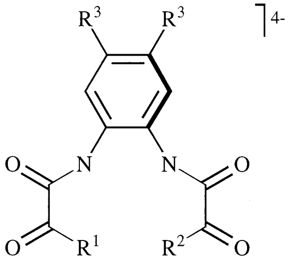

R^1	R^2	R^3	Ligand	E/V vs. SCE
O	O	H	opba (**18**)	0.41[a]
O	NCH_3	H	mopba (**19**)	0.12
NCH_3	NCH_3	H	dmopba (**20**)	−0.02
NCH_3	NCH_3	CH_3	dmopbaMe$_2$(**21**)	−0.05
NCH_3	NCH_3	Cl	dmopbaCl$_2$(**22**)	0.12
NCH_3	NCH_3	NO_2	dmopba(NO_2)$_2$(**23**)	0.15

[a] Irreversible couple.

5.2. High-valent nickel and cobalt complexes with bis(disubstituted)oxamides

Focusing on the electrochemistry of **20** with later first row transition metal ions (Table 7 and Fig. 33), the diamagnetic low-spin square-planar nickel(II) complex $[Ni(dmopba)]^{2-}$ experiences not only one but two reversible one-electron redox processes. The first one corresponds to the nickel(II)/nickel(III) oxidation, while the second one can be tentatively assigned to the nickel(III)/nickel(IV) oxidation, even if a ligand-centered oxidation leading to a Ni(III)-organic radical species cannot be definitively discarded. In fact, the square-planar copper(II) complex $[Cu(dmopba)]^{2-}$ mentioned above also shows a second but completely irreversible

Table 7

Values of the redox potentials (vs. SCE) for the later first row transition metal complexes of the bis(disubstituted oxamido) ligand dmopba (acetonitrile, 25°C, 0.1 mol dm^{-3} NEt_4ClO_4)

		M		
E_n	Redox couple	Cu	Ni	Co
E_1	$[ML]^-/[ML]^{2-}$	−0.02	0.13	−0.52
E_2	$[ML]/[ML]^-$	1.13[a]	0.90	0.03

[a] Irreversible couple.

oxidation at relatively high potentials which undoubtedly corresponds to the oxidation of the benzene ring from the dmopba ligand. A similar situation is observed for the paramagnetic intermediate-spin ($S = 1$) square-planar cobalt(III) complex [Co(dmopba)]$^-$, which shows a reversible one-electron reversible reduction to the corresponding cobalt(II) complex, together with a reversible one-electron oxidation to a formally cobalt(IV) species.

Finally, it deserves to be noted that the redox potentials for the metal centered M(III)/M(II) process along this series follow the trend cobalt $<$ copper $<$ nickel as illustrated in Fig. 33. However, the attainment of the trivalent state for the copper complex is expected to be much more difficult compared to that of nickel, essentially owing to the larger value of the third ionization energy. This anomalous behaviour for the copper case is explained in terms of the greater gain in the crystal field stabilization energy in a square-planar environment for the Cu(III)/Cu(II) redox change with respect to the Ni(III)/Ni(II) process.

On the other hand, the corresponding nickel and cobalt complexes of dmopba and the related mopba and opba ligands are efficient homogeneous catalysts for the aerobic epoxidation of olefins with co-oxidation of pivalaldehyde to pivalic acid [91,92]. The modulation of the catalytic activity by substituents along these series of metal complexes points out the role of high-valent metal(IV)-oxo species as the putative intermediates in these oxygen atom transfer reactions (16,17).

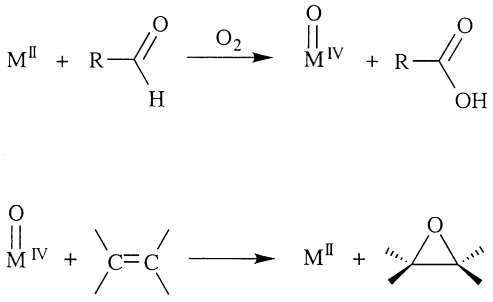

(16,17)

In general, discrete M=O groups are not expected to be stable under ordinary conditions for any transition metal beyond iron [93]; however, the Ni^{IV}=O and Co^{IV}=O species may be capable of transistory existence when supported by tetraanionic polychelating oxidative resistant ligands with large donor capacities such as this family of bis(disubstituted oxamides).

6. Conclusions

In the present review, we have illustrated the great versatility as ligands of the *N*,*N*′-substituted oxamides. These organic pendant arms allow the chemist to overcome both the insolubility of the oxamide in common solvents and the easy hydrolysis it undergoes in the presence of metal ions and also to improve its coordinating capability because the occurrence of six- and/or five-membered fused chelate rings. Simple organic reactions allow the preparation of symmetric and asymmetric *N*,*N*′-substituted oxamides which can adopt *cis* and *trans* conformations in their metal complexes depending on different factors such as the steric hindrance, metal to oxamidate metal ratio, presence of coligands, etc. Studies of complex formation in water allowed the determination of the stability constants of the existing species in solution and showed the best experimental conditions to prepare the desired mono- and polynuclear species. The nuclearity of the polynuclear compound can be increased stepwise by using the stable mononuclear copper(II) complex as building block (complex as ligand strategy) towards other metal ions or performed complexes. Moreover, the strong basicity of the deprotonated amido–nitrogen atoms is able to stabilize high oxidation states in their complexes with late transition metal ions, the resulting high valent species appearing as active oxidizing agents for the aerobic epoxidation of olefins. Finally, bimetallic oxamidato-bridged compounds are well known in magnetochemistry because they are suitable candidates in designing molecular-based magnets [17,61–65,94–101]. This very interesting application of the oxamidato complexes is not covered in the present report for brevity reasons and it certainly deserves a further review taking as basis the coupled solution and solid state studies that we have summarized here above.

Acknowledgements

Financial support from the Spanish DGICYT and the French–Spanish Integrated Actions through research projects and fellowships is gratefully acknowledged. Our deepest gratitude is also extended to great number of coworkers and colleagues from different countries whose enthusiastic and competent work contribute to create the scientific knowledge which is summarized herein. Their names are listed in the quoted references. The authors wish to point out that without them, this work would not be.

References

[1] K.A. Hoffmann, U. Ehrardt, Ber. 46 (1913) 1457.
[2] M. Rising, J.S. Hicks, G.A. Moarke, J. Biol. Chem. 89 (1930) 1.
[3] N.S. Poddubnaya, N.L. Gabrilov, Z. Obshck. Khim. 18 (1948) 1848.
[4] Y. Kuroda, M. Kato, K. Sone, Bull. Chem. Soc. Jpn. 34 (1961) 877.
[5] P.X. Armendarez, K. Nakamoto, Inorg. Chem. 5 (1966) 796.
[6] K. Nonoyama, Doctoral Thesis, Gakushūin University, Tokyo, No. 43, 1985.
[7] K. Nonoyama, H. Ojima, K. Ohki, M. Nonoyama, Inorg. Chim. Acta 41 (1980) 155.
[8] J. Sletten, Acta Chem. Scand. A36 (1982) 345.
[9] J. Sletten, Acta Chem. Scand. A39 (1985) 475.
[10] A. Bencini, C. Benelli, D. Gatteschi, C. Zanchini, A.C. Fabretti, G.C. Franchini, Inorg. Chim. Acta 86 (1984) 169.
[11] M. Verdaguer, O. Kahn, M. Julve, A. Gleizes, Nouv. J. Chim. 9 (1985) 325.

[12] L. Soto, J. García, E. Escrivá, J.-P. Legros, J.-P. Tuchagues, F. Dahan, A. Fuertes, Inorg. Chem. 28 (1989) 3378.

[13] H. Okawa, N. Matsumoto, M. Koikawa, K. Takeda, S. Kida, J. Chem. Soc. Dalton Trans. (1990) 1383.

[14] J.J. Bour, P.J.M.W.L. Birker, J.J. Steggerda, Inorg. Chem. 10 (1971) 1202.

[15] H. Ojima, K. Nonoyama, Coord. Chem. Rev. 92 (1980) 85.

[16] Y. Pei, K. Nakatani, O. Kahn, J. Sletten, J.P. Renard, Inorg. Chem. 28 (1989) 3170.

[17] Y. Pei, O. Kahn, K. Nakatani, E. Codjovi, C. Mathonière, J. Sletten, J. Am. Chem. Soc. 113 (1993) 6558.

[18] H. Sigel, R.B. Martin, Chem. Rev. 82 (1982) 385.

[19] F. Lloret, M. Julve, J. Faus, Y. Journaux, M. Philoche-Levisalles, Y. Jeannin, Inorg. Chem. 28 (1989) 3702.

[20] F. Lloret, J. Sletten, R. Ruiz, M. Julve, J. Faus, M. Verdaguer, Inorg. Chem. 31 (1992) 778.

[21] F. Lloret, M. Julve, J. Faus, R. Ruiz, I. Castro, M. Mollar, M. Philoche-Levisalles, Inorg. Chem. 31 (1992) 784.

[22] F. Lloret, M. Julve, J.A. Real, J. Faus, R. Ruiz, M. Mollar, I. Castro, C. Bois, Inorg. Chem. 31 (1992) 2956.

[23] J.A. Real, M. Mollar, R. Ruiz, J. Faus, F. Lloret, M. Julve, M. Philoche-Levisalles, J. Chem. Soc. Dalton Trans. (1993) 1483.

[24] A.E. Martell, R.M. Smith, Critical Stability Constants, vols. 1–6, Plenum, New York, 1989.

[25] F. Sprta, M. Bartusek, Collect. Czech. Chem. Commun. 39 (1974) 2023.

[26] K. Kahman, H. Sigel, H. Erlenmeyer, Helv. Chim. Acta 47 (1964) 1754.

[27] J.A. Pople, R.K. Nesbet, J. Chem. Phys. 27 (1954) 571.

[28] M.J. Frisch, J.S. Binkley, H.B. Schlegel, K. Raghavachari, C.F. Melius, R.L. Martin, J.J.P. Stewart, F.W. Bobrowicz, C.M. Rohlfing, L.R. Kahn, D.J. Defrees, R. Seeger, R.A. Whitside, D.J. Fox, E.M. Fluder, J.A. Pople, Gaussian 86, Carnegie-Mellon Quantum Chemistry, Pittsburg, PA, 1984.

[29] P. Gans, A. Sabatini, A. Vaca, J. Chem. Soc. Dalton Trans. (1985) 1195.

[30] A.E. Martell, R.J. Motekaitis, The Determination and Use of Stability Constants, VCH, New York, 1988.

[31] R. Ruiz, F. Lloret, M. Julve, M. Philoche-Levisalles, C. Bois, (unpublished).

[32] Z.N. Chen, W.X. Tang, K.B. Yu, Polyhedron 13 (1994) 783.

[33] Y. Journaux, J. Sletten, O. Kahn, Inorg. Chem. 25 (1986) 439.

[34] J.L. Sanz, B. Cervera, R. Ruiz, C. Bois, J. Faus, F. Lloret, M. Julve, J. Chem. Soc. Dalton Trans. (1988) 1359.

[35] J.P. Laurent, J.P. Costes, G. Pradié, Inorg. Chim. Acta 213 (8) (1993) 57.

[36] K. Nonoyama, H. Ojima, M. Nonoyama, Inorg. Chim. Acta 20 (1976) 127.

[37] K. Nonoyama, H. Ojima, M. Nonoyama, Inorg. Chim. Acta 59 (1982) 275.

[38] A.C. Fabretti, A. Giusti, V.G. Albano, C. Castellari, D. Gatteschi, R. Sessoli, J. Chem. Soc. Dalton Trans. (1991) 2133.

[39] P.R. Wei, L. Jia, C.R. Liu, Q. Han, G.C. wei, S. Gao, Polyhedron 14 (1995) 441.

[40] H. Okawa, Y. Kawahara, M. Mikuriya, S. Kida, Bull. Chem. Soc. Jpn. 53 (1980) 549.

[41] F. Lloret, Y. Journaux, M. Julve, Inorg. Chem. 29 (1990) 3967.

[42] J.L. Sanz, R. Ruiz, A. Gleizes, F. Lloret, J. Faus, M. Julve, J.J. Borrás-Almenar, Y. Journaux, Inorg. Chem. 35 (1996) 7384.

[43] H. Ojima, K. Nonoyama, Z. Anorg. Allg. Chem. 429 (1977) 282.

[44] Z.Y. Zhang, D.Z. Liao, Z.H. Jiang, S.Q. Hao, X.Q. Hao, X.K. Yao, H.G. Wang, Inorg. Chim.Acta 173 (1990) 201.

[45] J. Ribas, A. García, M. Monfort, Polyhedron 10 (1991) 1785.

[46] Z.M. Liu, D.Z. Liao, Z.H. Jiang, G.L. Wang, Synth. React. Inorg. Met.-Org.Chem. 21 (1991) 289.

[47] Z.M. Liu, Z.H. Jiang, D.Z. Liao, G.L. Wang, X.K. Yao, H.G. Wang, Acta Chim. Sin. 49 (1991) 981.

[48] A. Escuer, R. Vicente, J. Ribas, R. Costa, X. Solans, Inorg. Chem. 31 (1992) 2627.

[49] R. Ruiz, F. Lloret, M. Julve, J. Faus, M.C. Muñoz, X. Solans, Inorg. Chim. Acta 213 (1993) 261.

[50] C. Mathonière, O. Kahn, J.C. Daran, H. Hilbig, F.H. Köhler, Inorg. Chem. 32 (1993) 4057.
[51] Y. Journaux, J. Sletten, O. Kahn, Inorg. Chem. 24 (1985) 4063.
[52] J.M. Domínguez-Vera, J.M. Moreno, N. Gálvez, J.S. Suárez-Varela, E. Colacio, R. Kivekas, M. Klinge, Inorg. Chim. Acta 281 (1998) 95.
[53] M. Mollar, R. Ruiz, F. Lloret, M. Julve, Y. Journaux, M. Philoche-Levisalles (unpublished results).
[54] J.A. Real, R. Ruiz, J. Faus, F. Lloret, M. Julve, Y. Journaux, M. Philoche-Levisalles, C. Bois, J. Chem. Soc. Dalton Trans. (1994) 3769.
[55] A. Yoshino, W. Nowacki, Z. Krystallogr. 139 (1974) 337.
[56] H. Ojima, K. Yamada, Bull. Chem. Soc. Jpn. 43 (1970) 3018.
[57] J.A. Real, J. Cano, R. Ruiz, C. Bois, J. Faus, F. Lloret, M. Julve (unpublished results).
[58] L.G. Sillén, A.E. Martell, Stability Constants of Metal-Ion Complexes, Suppl. No. 1, The Chemical Society, Oxford, England, 1971.
[59] J. Votava, J. Havel, M. Bartusek, Chem. Zvesti 29 (1975) 734.
[60] R. Ruiz, Ph. D. Thesis, University of València, 1995.
[61] K. Nakatani, J.Y. Carriat, Y. Journaux, O. Kahn, F. Lloret, J.P. Renard, Y. Pei, J. Sletten, M. Verdaguer, J. Am. Chem. Soc. 111 (1989) 5739.
[62] Y. Pei, O. Kahn, J. Sletten, J.P. Renard, R. Georges, J.C. Gianduzzo, J. Curély, Q. Xu, Inorg. Chem. 27 (1988) 47.
[63] F. Lloret, M. Julve, R. Ruiz, Y. Journaux, K. Nakatani, O. Kahn, J. Sletten, Inorg. Chem. 32 (1993) 27.
[64] R. Ruiz, C. Surville-Barland, Y. Journaux, J.C. Colin, I. Castro, B. Cervera, M. Julve, F. Lloret, F. Sapiña, Chem. Mater. 9 (1997) 201.
[65] C. Surville-Barland, R. Ruiz, A. Aukauloo, Y. Journaux, I. Castro, B. Cervera, M. Julve, F. Lloret, F. Sapiña, Inorg. Chim. Acta 278 (1998) 159.
[66] R. Ruiz, B. Cervera, F. Lloret, M. Julve, Y. Journaux (unpublished results).
[67] J.C. Colin, T. Mallah, Y. Journaux, M. Mollar, F. Lloret, M. Julve, K. Boubekeur, Inorg. Chim. Acta 246 (1996) 249.
[68] MMX derived from MM2 (QCPE-395, 1977) of NL Allinger.
[69] J.M. Lehn, J.P. Sauvage, J. Am. Chem. Soc. 97 (1975) 6700.
[70] J.M. Lehn, Angew. Chem. Int. Ed. Engl. 27 (1988) 89.
[71] T.M. Garret, T.J. Mc Murry, M.W. Hosseini, Z.E. Reyes, F.E. Hahn, K.N. Raymond, J. Am. Chem. Soc. 113 (1991) 2965.
[72] J.C. Colin, T. Mallah, Y. Journaux, F. Lloret, M. Julve, C. Bois, Inorg. Chem. 35 (1996) 4170.
[73] J. Soto, R. Martínez-Máñez, J. Payá, F. Lloret, M. Julve, Transit. Met. Chem. 18 (1992) 1993.
[74] T.F. Collins, Acc. Chem. Res. 27 (1994) 279 and references therein.
[75] K. Nag, A. Chakravorty, Coord. Chem. Rev. 33 (1980) 87.
[76] K. Nakatani, J. Sletten, S. Halut-Desporte, S. Jeannin, Y. Jeannin, O. Kahn, Inorg. Chem. 30 (1991) 164.
[77] R. Ruiz, C. Surville-Barland, A. Aukauloo, E. Anxolabehere-Mallart, Y. Journaux, J. Cano, M.C. Muñoz, J. Chem. Soc. Dalton Trans. (1997) 745.
[78] B. Cervera, J.L. Sanz, M.J. Ibáñez, G. Vila, F. Lloret, M. Julve, R. Ruiz, X. Ottenwaelder, A. Aukauloo, S. Poussereau, Y. Journaux, M.C. Muñoz, J. Chem. Soc. Dalton Trans. (1998), 781.
[79] P.J.M.W.L. Birker, J. Chem. Soc. Chem. Commun. (1977) 444.
[80] L.L. Diaddario, W.R. Robinson, D.W. Margerum, Inorg. Chem. 22 (1983) 1021.
[81] F.C. Anson, T.J. Collins, T.G. Richmond, B.D. Santarsiero, J.E. Toth, B.G.R.T. Treco, J. Am. Chem. Soc. 109 (1987) 2974.
[82] W.E. Keys, J.B.R. Dunn, T.M.J. Loehr, J. Am. Chem. Soc. 99 (1977) 4527.
[83] B.R. Serr, C.E.L. Headford, C.M. Elliot, O.P. Anderson, Acta Cryst. C46 (1990) 500.
[84] M.R. Caira, K.R. Koch, C. Sacht, Acta Cryst. C47 (1991) 26.
[85] T.M. Yao, X.Z. You, C. Li, L.F. Li, Q.C. Yang, Acta Cryst. C50 (1994) 67.
[86] J. Hanss, H.J. Krüger, Angew. Chem. Int. Ed. Engl. 35 (1996) 2827.
[87] D.W. Margerum, K.L. Chellapa, F.P. Bossu, G.L. Burce, J. Am. Chem. Soc. 97 (1975) 6894.
[88] F.P. Bossu, K.L. Chellapa, D.W. Margerum, J. Am. Chem. Soc. 99 (1977) 2195.

[89] L. Fabbrizzi, A. Perotti, A. Poggi, J. Chem. Soc. Chem. Commun. (1980) 646.
[90] L. Fabbrizzi, A. Poggi, Inorg. Chem. 22 (1983) 1411.
[91] J. Estrada, I. Fernández, J.R. Pedro, X. Ottenwaelder, R. Ruiz, Y. Journaux, Tetrahedron Lett. 38 (1997) 2377.
[92] I. Fernández, J.R. Pedro, A.L. Roselló, R. Ruiz, X. Ottenwaelder, Y. Journaux, Tetrahedron Lett. 39 (1998) 2869.
[93] R.H. Holm, Chem. Rev. 87 (1987) 1401.
[94] O. Kahn, Y. Pei, M. Verdaguer, J.P. Renard, J. Sletten, J. Am. Chem. Soc. 110 (1988) 782.
[95] O. Kahn, Y. Pei, K. Nakatani, Y. Journaux, J. Sletten, New J. Chem. 16 (1992) 269.
[96] H.O. Stumpf, Y. Pei, O. Kahn, J. Sletten, J.P. Renard, J. Am. Chem. Soc. 111 (1993) 6738.
[97] O. Kahn, Molecular Magnetism, VCH, 1993.
[98] O. Kahn, Adv. Inorg. Chem. 43 (1995) 179.
[99] O. Kahn, Y. Journaux, C. Mathonière, in: O. Kahn (Ed.), Magnetism: A Supramolecular Function, Kluwer Academic, Dordrecht, Netherlands, 1996, pp. 531.
[100] O. Kahn, in: E. Coronado, P. Delhaès, D. Gatteschi, J.S. Miller (Eds.), Molecular Magnetism: From Molecular Assemblies to the Devices, Kluwer Academic, Dordrecht, Netherlands, 1996, pp. 243.
[101] O. Cador, D. Price, J. Larionova, C. Mathonière, O. Kahn, J.V. Yahmi, J. Mater. Chem. 7 (1997) 1263.